Generalizing Robust Control Barrier Functions From a Controller Design Perspective

ANIL ALAN [1] **(Student Member, IEEE), TAMAS G. MOLNAR** [2] **(Member, IEEE),**
AARON D. AMES [3] **(Fellow, IEEE), AND GÁBOR OROSZ** [1,4] **(Senior Member, IEEE)**

[1]Department of Mechanical Engineering, University of Michigan, Ann Arbor, MI 48109 USA
[2]Department of Mechanical Engineering, Wichita State University, Wichita, KS 67260 USA
[3]Department of Mechanical and Civil Engineering, California Institute of Technology, Pasadena, CA 91125 USA
[4]Department of Civil and Environmental Engineering, University of Michigan, Ann Arbor, MI 48109 USA

CORRESPONDING AUTHOR: ANIL ALAN (e-mail: anilalan@umich.edu).

ABSTRACT While control barrier functions provide a powerful tool to endow controllers with formal safety guarantees, robust control barrier functions (RCBF) can be used to extend these guarantees for systems with model inaccuracies. This paper presents a generalized RCBF framework that unifies and extends existing notions of RCBFs for a broad class of model uncertainties. Main results are conditions for robust safety through generalized RCBFs. We apply these generalized principles for more specific design examples: a worst-case type design, an estimation-based design, and a tunable version of the latter. These examples are demonstrated to perform increasingly closer to an oracle design with ideal model information. Theoretical contributions are demonstrated on a practical example of a pendulum with unknown periodic excitation. Using numerical simulations, a comparison among design examples are carried out based on a performance metric depicting the increased likeness to the oracle design.

INDEX TERMS Control barrier function, model uncertainty, robust safety, safe control, safety filter.

I. INTRODUCTION

Safety is one of the most important requirements when designing an autonomous system. Motivated to find control inputs with formal safety certification, safety-critical controllers can be designed using methods such as model predictive control [1], reference governor [2], or Hamilton-Jacobi-based reachability [3]. Relying on a safety verification tool called barrier certificates [4], control barrier functions (CBFs) provide one such framework, and this has been widely adopted in the recent literature [5], [6]. In simple terms, safety (or set invariance) is defined by staying in safe states corresponding to the positive values of a scalar-valued function h. The CBF framework provides a sufficient condition for safe control in the form of a lower bound on the time derivative $\dot{h}$. One of the widely utilized applications of CBFs has been a control design paradigm called *safety filters* [6], [7], where the deviation from a given controller is penalized in a quadratic program (QP) while subject to a CBF-based safety constraint.

Proven to be a powerful tool in synthesizing safe controllers, the CBF literature has expanded towards various directions, including higher order derivatives to increase feasibility [8], [9], sampled-time systems [10], [11], [12], different time-explicit safety definitions [13], [14], and more general temporal logic specifications [15]. One particular research direction that has gathered much interest is robustness against unmodeled dynamics. CBF-based safety guarantees may degrade if there is a mismatch between the real system and the model used to represent it. This mismatch may emerge from unknown external disturbances [16] or complex internal dynamics omitted to facilitate the implementation.

Two main approaches have arisen for robustness against deterministic uncertainties: input-to-state safety (ISSf) and robust control barrier functions (RCBFs). On one hand, the ISSf framework (which is inspired from input-to-state stability for control Lyapunov functions [17]) can be used to obtain an arbitrarily small (graceful) degradation of safety guarantees in the presence of uncertainty [16], [18], [19], [20]. On the

other hand, motivated to obtain zero safety degradation, the RCBF framework investigates conditions to *sufficiently* ensure the CBF-based safety condition for systems with uncertainty under the worst possible case [21].

This paper advances the theoretical and practical understanding of RCBFs by generalizing their framework to accommodate a wide spectrum of uncertainties. In particular, we present an overview of the sufficient conditions for feasible robust safety-critical control against different forms of uncertainties. Then, we study solutions for specific problem setups with increasing likeness to an oracle controller. Robust safety filters designed based on these principles are implemented on a practical example, and we illustrate the theoretical findings using simulations.

A. LITERATURE ON RCBF

The study of robust optimization in the presence of uncertainty spans back to earlier studies [22], [23], even in the context of barrier-Lyapunov functions [24]. One of the key contributions for the CBF-based controllers was given in [21], where the CBF-based safety constraint was modified, hence the name *robust CBF (RCBF)*. Providing conditions for sufficiently compensating the uncertainty under the worst-case scenario, the RCBF framework proves to be an effective method to guarantee robust safety. The RCBF framework received attention so much so the definition has expanded rapidly to other types of uncertainties ever since. For example, uncertainties with state dependence were addressed in the form of parametric uncertainties [25], [26], [27], or in a more general form [13], [28], [29]. The more challenging case of uncertainties in how control inputs are related to the state dynamics were considered in works [30], [31], [32], [33].

The framework was also adopted by less conservative methods relying on estimators with deterministic or probabilistic residual estimation errors. RCBF definitions in these works took different forms to incorporate the estimator and the error compensation. For example, adaptive control techniques were adopted for parametric uncertainties [25], [26], [27], [34], where limitations in the parameter space were used in the RCBF definition. Various disturbance and state observer approaches were implemented for online uncertainty estimation [29], [35], [36], [37], [38], [39], [40], [41], where bounds on the Euclidean norm of the uncertainty, its derivative or its underlying dynamics were incorporated into the RCBF definition, and various forms of Lipschitz constants were utilized. Learning-based and data-driven extensions of the RCBF framework typically utilize Lipschitz constants or bounded Jacobians regarding the uncertainty [42], [43], [44]. When unknown dynamics are estimated with probabilistic confidence bounds, adding these terms in the RCBF definition provides safety guarantees with high probability [45], [46], [47], [48], [49], [50].

Robustness requirements for deploying safety-critical controllers with specified sampling interval were also addressed within the RCBF framework. In this context, the definition of the RCBF incorporates the Lipschitz constants of the system

and constraint functions, along with the bounds of the control space [10], [11], [51]. Other types of imperfections addressed using the RCBF framework are robustness against measurement errors [52] and unmodeled input dynamics [53], which utilize Lipschitz constant and integral quadratic constraints, respectively. The RCBF framework was also extended to higher order CBF formulations [54], [55].

B. CONTRIBUTIONS

The aforementioned boom in the robust safety-critical control literature inevitably led to a fractured landscape of different RCBF definitions that rely on various assumptions on the system, safe set and uncertainty. Motivated by the lack of such a study, we present an overview of the general robust safety-critical control design principles within the scope of the CBF framework as the first contribution of the paper. In particular, we elevate the RCBF formulation by considering a general form of uncertainty. This generalization not only unifies existing approaches but also establishes a foundation for deriving simplified verification conditions and implementable solutions for robust safety-critical controllers.

The second contribution of the paper demonstrates the utility of the general framework by developing a robust safety filter for a previously unaddressed type of uncertainty. Specifically, we propose a novel sufficient condition to guarantee feasibility and robust safety and to enable the derivation of closed-form controllers in certain scenarios. Additionally, leveraging the generalized framework, we introduce a tunable controller design that incorporates disturbance observers, extending the state of the art by reducing conservativeness. The tunability concept, originally conceived for the ISSf framework, is adapted here to improve flexibility and performance, demonstrating its broad applicability across different RCBF methods.

Finally, the theoretical advancements are validated through application to a physics-based example involving a pendulum with unknown periodic excitation. Numerical simulations showcase the efficacy of the proposed methods, compare their performance metrics to an idealized oracle design and highlight the significant reduction in conservativeness achieved by the proposed controllers. These results underscore the potential of the generalized RCBF framework to unify, extend, and enhance existing approaches of robust safety-critical control.

C. ORGANIZATION

The paper is organized as follows. Section II provides the theoretical foundation, introducing the general principles of CBFs and extending these concepts to RCBFs to address system uncertainties. Section III presents the detailed design steps of a robust safety filter for a specific set of uncertainty assumptions. In Section IV we extend these principles for a less conservative problem setup with a disturbance observer. Section V introduces a detailed discussion on the performance of previously proposed controllers on a practical application platform. Section VI concludes the paper with a summary and future work.

II. GENERALIZED RCBF FRAMEWORK

A continuous function $\alpha : \mathbb{R} \to \mathbb{R}$ is called *extended class* $\mathcal{K}_\infty$ function (denoted as $\alpha \in \mathcal{K}_\infty^e$) if $\alpha(0) = 0$, it is strictly increasing, and $\lim_{r \to \pm\infty} \alpha(r) = \pm\infty$. The term $\nabla h : \mathbb{R}^n \to \mathbb{R}^n$ denotes the gradient vector of a function $h : \mathbb{R}^n \to \mathbb{R}$. Also, $\|\cdot\|$ denotes the 2-norm.

A. SAFETY AND CONTROL BARRIER FUNCTIONS

Consider a nonlinear system affine in control:

$$\dot{x} = f(x, t) + g(x, t)u, \quad x(t_0) = x_0 \in \mathbb{R}^n, \tag{1}$$

where terms $x \in \mathbb{R}^n$, $u \in \mathbb{U} \subseteq \mathbb{R}^m$ and $t \in \mathbb{T} \triangleq [t_0, \infty)$ denote the state, input and time from a given initial time $t_0 \in \mathbb{R}$, respectively, while functions $f : \mathbb{R}^n \times \mathbb{T} \to \mathbb{R}^n$ and $g : \mathbb{R}^n \times \mathbb{T} \to \mathbb{R}^{n \times m}$ describe dynamics. Substituting a feedback controller $k : \mathbb{R}^n \times \mathbb{T} \to \mathbb{R}^m$ into the input $u = k(x, t)$ leads to the closed loop system:

$$\dot{x} = f(x, t) + g(x, t)k(x, t). \tag{2}$$

If we can find an open set $\mathbb{X} \subset \mathbb{R}^n$ on which functions f, g and k are locally Lipschitz continuous in x and piece-wise continuous in t for all $t \in \mathbb{T}$, then there exists a time interval $I(x_0, t_0) \subseteq \mathbb{T}$ for each initial condition $x_0 \in \mathbb{X}$ such that (2) has a unique solution $x(t)$ for all $t \in I(x_0, t_0)$ [56]. Throughout the paper we assume that the solution is forward complete, that is, $I(x_0, t_0) = \mathbb{T}$.

Our goal is to obtain a formal guarantee that, initiated from a set, the solution never leaves the set.

Definition 1 (Safety, [6]): The closed loop system (2) is safe w.r.t. a set $\mathcal{S} \subset \mathbb{X} \subset \mathbb{R}^n$ if for all $x_0 \in \mathcal{S}$ we have that $x(t) \in \mathcal{S}$ for all $t \geq t_0$.

In particular, we consider set $\mathcal{S}$ defined as the 0-superlevel set of a continuously differentiable function $h : \mathbb{X} \to \mathbb{R}$:

$$\mathcal{S} = \left\{ x \in \mathbb{X} \subset \mathbb{R}^n \mid h(x) \geq 0 \right\}, \tag{3}$$

$$\partial\mathcal{S} = \left\{ x \in \mathbb{X} \subset \mathbb{R}^n \mid h(x) = 0 \right\}, \tag{4}$$

$$\text{Int}(\mathcal{S}) = \left\{ x \in \mathbb{X} \subset \mathbb{R}^n \mid h(x) > 0 \right\}. \tag{5}$$

Here, $\partial\mathcal{S}$ and $\text{Int}(\mathcal{S})$ denote the boundary and the interior of $\mathcal{S}$, respectively.

Definition 2 (Regular value): A number $p \in \mathbb{R}$ is called a *regular value of the function* $h : \mathbb{X} \to \mathbb{R}$ if for each $x_p \in \mathbb{X}$ satisfying $h(x_p) = p$ we have $\nabla h(x_p) \neq 0$.

If 0 is a regular value of h, then a non-zero gradient exists for h everywhere on $\partial\mathcal{S}$. Then a vector $y \in \mathbb{R}^n$ is an element of the tangent cone of $\mathcal{S}$ at a point $x \in \partial\mathcal{S}$ if we have $\nabla h(x)^\top y \geq 0$ [57]. Nagumo's theorem provide a condition for safety by utilizing tangent cones [58], [59]:

Theorem 1 (Nagumo's theorem, [58]): Let $\mathcal{S}$ be the 0-superlevel set defined as in (3) with a continuously differentiable function $h : \mathbb{X} \to \mathbb{R}$, and let 0 be a regular value of h. The closed loop system (2) is safe w.r.t. $\mathcal{S}$ if and only if:

$$\nabla h(x)^\top (f(x, t) + g(x, t)k(x, t)) \geq 0, \ \forall (x, t) \in (\partial\mathcal{S} \times \mathbb{T}). \tag{6}$$

Remark 1: A proof of Nagumo's theorem is in [57, §4.2]. While this proof is constructed for autonomous systems, it can be extended to nonautonomous ones by introducing the time variable as a fictitious state; see [57, §4.2.2] for details.

Our overarching goal is to design safety-critical controllers $k(x, t)$ such that the corresponding closed loop system (2) is safe. *Control barrier functions* provide a sufficient condition for the existence of a safe controller. Note that, hereafter we will utilize the Lie derivative notation $L_f h$ and $L_g h$ for the time derivative of h along the system:

$$\dot{h}(x, u, t) = \underbrace{\nabla h(x)^\top f(x, t)}_{L_f h(x, t)} + \underbrace{\nabla h(x)^\top g(x, t)}_{L_g h(x, t)} u. \tag{7}$$

Definition 3 (Control barrier function [60]): Let $\mathcal{S}$ be the 0-superlevel set defined as in (3) with a continuously differentiable function $h : \mathbb{X} \to \mathbb{R}$, and let 0 be a regular value of h. Then, the function h is called a *control barrier function (CBF)* for (1) on $(\mathbb{X} \times \mathbb{T})$ if there exists a $\alpha \in \mathcal{K}_\infty^e$ such that $\forall (x, t) \in (\mathbb{X} \times \mathbb{T})$:

$$\sup_{u \in \mathbb{U}} \left[L_f h(x, t) + L_g h(x, t)u \right] > -\alpha(h(x)). \tag{8}$$

Defining the point-wise set of controllers:

$$K_{\text{CBF}}(x, t) \triangleq \{u \in \mathbb{U} \mid L_f h(x, t) + L_g h(x, t)u \geq -\alpha(h(x))\}, \tag{9}$$

the existence of h implies that $K_{\text{CBF}}(x, t)$ is not empty $\forall (x, t) \in (\mathbb{X} \times \mathbb{T})$. Safety is ensured for controllers taking values in K_{CBF}.

Lemma 1 ([60]): Let h be a CBF for (1) on $(\mathbb{X} \times \mathbb{T})$. A controller $k(x, t)$, that is Lipschitz continuous in x and piece-wise continuous in t, ensures that the system (2) is safe w.r.t. $\mathcal{S} \subset \mathbb{X}$ if $k(x, t) \in K_{\text{CBF}}(x, t)$ holds $\forall (x, t) \in (\mathbb{X} \times \mathbb{T})$.

Proof: The $\mathcal{K}_\infty^e$ definition implies $\alpha(h(x)) = 0$, $\forall x \in \partial\mathcal{S}$. Thus, (9) implies that any controller $k(x, t) \in K_{\text{CBF}}(x, t)$ satisfies (6). The regularity conditions on the controller k ensure the existence of a unique solution $x(t)$, and Theorem 1 completes the proof. ∎

Remark 2: In Definition 3 we look for a strict inequality in the condition (8), whereas the inequality is non-strict in the definition of K_{CBF} in (9). As elaborated in the works [5], [21], [59], [61], the strict inequality in the CBF definition allows us to endow the CBF-based controllers with useful properties such as continuity and Lipschitz continuity.

The following set definition will keep the notation compact throughout the paper:

$$\mathcal{G} = \{(x, t) \in (\mathbb{X} \times \mathbb{T}) \mid L_g h(x, t) = 0\}. \tag{10}$$

The set $\mathcal{G}$ contains x and t values that the vector valued function $L_g h(x, t)^\top \in \mathbb{R}^m$ vanishes. That is, the input relative degree of h becomes more than one for any $(x, t) \in \mathcal{G}$.

Remark 3 ([59]): The condition

$$L_f h(x, t) > -\alpha(h(x)), \ \forall (x, t) \in \mathcal{G}, \tag{11}$$

is a *necessary condition* for the inequality (8). This implies that, should (8) hold, then safety can be shown with $L_f h$ when the input relative degree of h is more than one. Furthermore,

if $\mathbb{U} = \mathbb{R}^m$, then (11) amounts to a *necessary and sufficient* condition to verify whether a function h is CBF [59]. This is an easier condition to check whether a given h is a CBF for a system. We will utilize this property to obtain simpler sufficient conditions that ensure the feasibility of the robust safety-critical control problem.

B. SAFETY FILTERS

We can utilize CBFs in a pointwise optimization problem under the context of *correcting a given–possibly unsafe– nominal controller*. In particular, the goal is to ensure safety in a minimally invasive fashion. Consider the controller

$$k_{\text{QP}}(x, t) = \underset{u \in \mathbb{U}}{\operatorname{argmin}} \quad \|u - k_{\text{d}}(x, t)\|^2$$

$$\text{s.t.} \qquad L_f h(x, t) + L_g h(x, t) u \geq -\alpha(h(x)). \tag{12}$$

Here $k_{\text{d}} : \mathbb{X} \times \mathbb{T} \to \mathbb{U}$ is an existing controller, Lipschitz continuous in x and piecewise continuous in t, with desired guarantees like optimality and stability. The constraint ensures safety, while the cost function penalizes the deviation from k_{d}. As a result, a minimum intervention occurs only when necessary (i.e., when $k_{\text{d}}(x, t) \notin K_{\text{CBF}}(x, t)$). If $\mathbb{U}$ can be represented with affine constraints, this problem becomes quadratic programming (QP). The following theorem summarizes key points about this CBF-based controller scheme (often referred to as *safety filter*).

Theorem 2 ([59], [62]): Let $\mathcal{S}$ be the 0-superlevel set defined as in (3) with a continuously differentiable function $h : \mathbb{X} \to \mathbb{R}$, and let 0 be a regular value of h.

- If $\mathbb{U} = \mathbb{R}^m$, then h is a CBF for (1) on $(\mathbb{X} \times \mathbb{T})$ if and only if (11) holds.
- Let h be a CBF for (1) on $(\mathbb{X} \times \mathbb{T})$, then the QP (12) is feasible, and $k_{\text{QP}}(x, t) \in K_{\text{CBF}}(x, t)$ for all $(x, t) \in (\mathbb{X} \times \mathbb{T})$. This implies that the system (2) is safe w.r.t. $\mathcal{S}$ when $u = k_{\text{QP}}(x, t)$.
- If $\mathbb{U} = \mathbb{R}^m$, then the QP has a closed-form solution:

$$k_{\text{QP}}(x, t) = k_{\text{d}}(x, t) + \max\left\{0, \overline{\Phi}(x, t)\right\} L_g h(x, t)^\top, \tag{13}$$

where the function $\overline{\Phi} : \mathbb{X} \times \mathbb{T} \to \mathbb{R}$ is defined as:

$$\overline{\Phi}(x, t) \triangleq \begin{cases} \Phi(x, t) & \text{if } L_g h(x, t) \neq 0, \\ 0 & \text{if } L_g h(x, t) = 0, \end{cases} \tag{14}$$

with the function $\Phi : \mathbb{X} \times \mathbb{T} \to \mathbb{R}$ given as:

$$\Phi(x, t) \triangleq -\frac{L_f h(x, t) + L_g h(x, t) k_{\text{d}}(x, t) + \alpha(h(x))}{\|L_g h(x, t)\|^2}. \tag{15}$$

Interested reader is referred to works for details [62], [63].

Remark 4: ([62], [63]) For a scalar input system, i.e., $m = 1$, the safety filter (13) simplifies to:

$$k_{\text{QP}}(x, t) = \begin{cases} \min\{k_{\text{d}}(x, t), \Phi_{\text{QP}}(x, t)\} & \text{if } L_g h(x, t) < 0, \\ \max\{k_{\text{d}}(x, t), \Phi_{\text{QP}}(x, t)\} & \text{if } L_g h(x, t) > 0, \\ k_{\text{d}}(x, t) & \text{if } L_g h(x, t) = 0, \end{cases} \tag{16}$$

where $\Phi_{\text{QP}} : \mathbb{X} \times \mathbb{T} \to \mathbb{R}$ is given as:

$$\Phi_{\text{QP}}(x, t) \triangleq -\frac{L_f h(x, t) + \alpha(h(x))}{L_g h(x, t)}. \tag{17}$$

Remark 5: Since the Lipschitz properties are preserved through a max/min operation [64], the safety filter in (13) (and (16)) can be shown to be Lipschitz continuous in x if all functions have the same property [21], [65].

Safety guarantees may degrade when the CBF-based control design relies on a partially known system model. Thus, successful implementation of a CBF-based safety-critical controller depends on the resilience of the design against uncertainties emerging from unmodeled dynamics. Next, we investigate conditions to obtain robust safety for the CBF-based safety condition (8) for a general type of uncertainty.

C. GENERALIZED ROBUST CBFS

Consider the system

$$\dot{x} = f(x, t) + g(x, t) u + \mu(x, u, t). \tag{18}$$

where f and g are the nominal (known) system functions, and $\mu : \mathbb{X} \times \mathbb{U} \times \mathbb{T} \to \mathbb{R}^n$ represents the uncertainty in the model. A controller k yields the closed loop system

$$\dot{x} = f(x, t) + g(x, t) k(x, t) + \mu(x, k(x, t), t). \tag{19}$$

Evaluating $\dot{h}$ along the open loop system (18) yields:

$$\dot{h}(x, u, t) = L_f h(x, t) + L_g h(x, t) u + L_\mu h(x, u, t). \tag{20}$$

The uncertainty prevents us from looking for the condition $\dot{h} \geq -\alpha(h)$, cf. (7). This motivates the introduction of robust control barrier functions (RCBFs) as follows. The main goal is to find a set of controllers $K_{\text{RCBF}}(x, t) \subseteq \mathbb{U}$ such that a controller $k(x, t) \in K_{\text{RCBF}}(x, t)$ implies the condition $\dot{h} \geq -\alpha(h)$ under the worst-case scenario. This goal can be achieved by modifying the condition (8) by introducing a compensation term, which will be denoted as σ in this paper.

The compensation term takes different forms based on what we know about the system and the uncertainty. For example, if there exists a $\overline{\mu} \geq 0$ such that $\|\mu(x, u, t)\| \leq \overline{\mu}$ for all $x \in \mathbb{X}$, $u \in \mathbb{U}$ and $t \geq t_0$, then we can use [21], [66]:

$$\sigma(x) = \overline{\mu} \|\nabla h(x)\|. \tag{21}$$

Consider that the uncertainty affects the system dynamics through input channels, that is, $\mu(x, u, t) = g(x, t) d(x, u, t)$. This case is called *matched uncertainty*. If the input uncertainty d satisfies $\|d(x, u, t)\| \leq \overline{d}$ with a $\overline{d} \geq 0$ for all $x \in \mathbb{X}$, $u \in \mathbb{U}$ and $t \geq t_0$, then, instead of (21), we can use:

$$\sigma(x, t) = \overline{d} \|L_g h(x, t)\|, \tag{22}$$

to scale the compensation with $L_g h(x, t)$ which characterizes the effect of d on $\dot{h}$. If $\|d(x, u, t)\| \leq \overline{d}_u \|u\|$ for all $x \in \mathbb{X}$, $u \in \mathbb{U}$ and $t \geq t_0$, which can occur if there is a sector-bounded uncertainty in the input [32], then one can use a compensation of the form

$$\sigma(x, t) = \overline{d}_u \|L_g h(x, t)\| \|u\|. \tag{23}$$

The input-to-state safety type of robust controllers utilize a robustifying function of the form [16], [18]:

$$\sigma_{\mathrm{ISSf}}(x, t) = \|L_g h(x, t)\|^2 \epsilon, \quad \epsilon > 0, \tag{24}$$

and

$$\sigma_{\mathrm{TISSf}}(x, t) = \|L_g h(x, t)\|^2 \epsilon(h(x)),$$

$$\epsilon(r) > 0, \quad \frac{\mathrm{d}\epsilon}{\mathrm{d}r}(r) \leq 0, \quad \forall r \in \mathbb{R}, \tag{25}$$

where the latter introduces the 'tunability'. Table I in [66] provides a summary of various forms of σ in the literature as well as the underlying assumptions on the uncertainty.

Definition 4 (Robust control barrier function, generalized from [21]): Let $\mathcal{S}$ be the 0-superlevel set defined as in (3) with a continuously differentiable function $h : \mathbb{X} \to \mathbb{R}$, and let 0 be a regular value of h. The function h is called a *robust control barrier function (RCBF)* for (18) on $(\mathbb{X} \times \mathbb{T})$ if there exist functions $\alpha \in \mathcal{K}^{\mathrm{e}}_{\infty}$ and $\sigma : \mathbb{X} \times \mathbb{U} \times \mathbb{T} \to \mathbb{R}$ such that

$$\sup_{u \in \mathbb{U}} \left[L_f h(x, t) + L_g h(x, t) u - \sigma(x, u, t) \right] > -\alpha(h(x)), \tag{26}$$

$\forall (x, t) \in (\mathbb{X} \times \mathbb{T})$.

Given a RCBF h with functions $\alpha \in \mathcal{K}^{\mathrm{e}}_{\infty}$ and σ, we can define the point-wise set of controllers:

$$K_{\mathrm{RCBF}}(x, t) \triangleq \{ u \in \mathbb{U} \mid$$

$$L_f h(x, t) + L_g h(x, t) u - \sigma(x, u, t) \geq -\alpha(h(x)) \}. \tag{27}$$

The following lemma summarizes the sufficient condition so that controllers from K_{RCBF} guarantee the robust safety:

Lemma 2: Let h be a RCBF for (18) on $(\mathbb{X} \times \mathbb{T})$ with a function σ. Any controller $k(x, t)$, that is locally Lipschitz continuous in x and piecewise continuous in t, satisfying $k(x, t) \in K_{\mathrm{RCBF}}(x, t)$ for all $(x, t) \in (\mathbb{X} \times \mathbb{T})$ ensures that the system (19) is safe w.r.t. $\mathcal{S}$ if the following condition holds for all $u \in K_{\mathrm{RCBF}}(x, t)$ and $(x, t) \in (\partial \mathcal{S} \times \mathbb{T})$

$$L_\mu h(x, u, t) + \sigma(x, u, t) \geq 0. \tag{28}$$

Proof: The $\mathcal{K}^{\mathrm{e}}_{\infty}$ definition implies $\alpha(h(x)) = 0$, $\forall x \in \partial \mathcal{S}$. Thus, it is evident from (27) and (28) that any controller $k(x, t) \in K_{\mathrm{RCBF}}(x, t)$ for all $(x, t) \in (\mathbb{X} \times \mathbb{T})$ ensures that (6) is satisfied. The regularity requirements on the controller k ensure the existence of a unique solution $x(t)$, and Theorem 1 completes the proof. ∎

In general, it is a challenging task to find a proper σ. For example, choosing a function that takes large positive values may satisfy the condition (28) conservatively. However, this decreases the feasibility of the control problem by making the set K_{RCBF} smaller, cf. (27). It is important to construct the compensation compatible with the safety problem (for example by adding ∇h or $L_g h$ into σ) and the uncertainty assumptions to mitigate this trade-off; see e.g. (21)–(23).

Furthermore, notice that the condition (28) is posed over the boundary of $\mathcal{S}$. Consequent to this observation, robust safety is primarily related to the values that the function σ takes

when $x \in \partial \mathcal{S}$. This gives us a certain relaxation factor that will be used in the 'tunable' setting in Section IV.

D. ROBUST SAFETY FILTERS

We can update the optimization problem (OP) in (12) based on the RCBF condition (26) to get the *robust safety filters:*

$$k_{\mathrm{OP}}(x, t) = \operatorname*{argmin}_{u \in \mathbb{U}} \quad \|u - k_{\mathrm{d}}(x, t)\|^2$$

$$\text{s.t.} \quad L_f h(x, t) + L_g h(x, t) u - \sigma(x, u, t) \geq -\alpha(h(x)), \tag{29}$$

where k_{d} is the desired controller. Relying on the RCBF definition and Lemma 2, we can summarize conditions such that k_{OP} ensures the closed-loop robust safety.

Theorem 3: Let h be a RCBF for (18) on $(\mathbb{X} \times \mathbb{T})$ with functions $\alpha \in \mathcal{K}^{\mathrm{e}}_{\infty}$ and σ. Then, the OP (29) is feasible, and $k_{\mathrm{OP}}(x, t) \in K_{\mathrm{RCBF}}(x, t)$ for all $(x, t) \in (\mathbb{X} \times \mathbb{T})$. Furthermore, the system (19) is safe w.r.t. $\mathcal{S}$ when $u = k_{\mathrm{OP}}(x, t)$ if k_{OP} is locally Lipschitz continuous in x and piecewise continuous in t, and σ satisfies (28) for all $u \in K_{\mathrm{RCBF}}(x, t)$ and $(x, t) \in (\partial \mathcal{S} \times \mathbb{T})$.

Proof: The existence of a RCBF implies that $K_{\mathrm{RCBF}}(x, t)$ is not empty for any $(x, t) \in (\mathbb{X} \times \mathbb{T})$, thus the constraint in (29) is feasible. Furthermore, this ensures $k_{\mathrm{OP}}(x, t) \in K_{\mathrm{RCBF}}(x, t)$ for all $(x, t) \in (\mathbb{X} \times \mathbb{T})$. Since σ satisfies (28), Lemma 2 concludes the proof. ∎

It is noted that the controller should have appropriate regularity properties for closed loop safety. Another design concern for σ is the implementation of the OP (29). In particular, the class of the OP depends on the structure of $\sigma(x, u, t)$ with respect to u. For example, if σ is affine in u, and $\mathbb{U}$ can be represented with affine constraints, then the problem remains a QP. Other functions can be put into other solution-friendly forms such as second order cone program (SOCP) [32], [67], or mixed-integer quadratic program [43].

III. IMPLEMENTATION OF GENERAL PRINCIPLES

In this section, we outline the design process for a novel safety filter tailored to address a specific set of uncertainty assumptions. We derive a sufficient condition to ensure feasibility and establish robust safety guarantees. Then we demonstrate the controller on an application.

A. WORST-CASE-BASED DESIGN

We start with the following assumption.

Assumption 1: The matrix $g(x, t)$ has full column rank for all $(x, t) \in (\mathbb{X} \times \mathbb{T})$, and thus the left pseudo-inverse $g^{\dagger} : \mathbb{X} \times \mathbb{T} \to \mathbb{R}^{m \times n}$ exists:

$$g^{\dagger}(x, t) = \left(g(x, t)^{\top} g(x, t) \right)^{-1} g(x, t)^{\top}. \tag{30}$$

Since the number of nonzero singular values of a matrix is equal to its rank, this assumption also implies that there exists a constant $\underline{\rho} > 0$ such that

$$\min_{i \in \{1, \dots, m\}} \rho_i(x, t) \geq \underline{\rho}, \quad \forall (x, t) \in (\mathbb{X} \times \mathbb{T}), \tag{31}$$

where $\rho_i(x, t)$ is the i-th singular value of $g(x, t)$ at any point $(x, t) \in (\mathbb{X} \times \mathbb{T})$.

Assumption 1 is common in disturbance rejection problems [68], [69]. Using the left pseudo-inverse $g^\dagger$, we can separate *matched* and *unmatched* uncertainties:

$$\mu(x, u, t) = g(x, t)d(x, u, t) + \Delta(x, u, t), \qquad (32)$$

where $d : \mathbb{X} \times \mathbb{U} \times \mathbb{T} \to \mathbb{R}^m$ is the uncertainty matched with input, and it is defined as:

$$d(x, u, t) \triangleq g^\dagger(x, t)\mu(x, u, t). \qquad (33)$$

The remaining term $\Delta : \mathbb{X} \times \mathbb{U} \times \mathbb{T} \to \mathbb{R}^n$ is called the unmatched uncertainty, where $g^\dagger(x, t)\Delta(x, u, t) = 0$ holds for all $x \in \mathbb{X}$, $u \in \mathbb{U}$ and $t \in \mathbb{T}$.

Consider the following assumption on how much the uncertainty can affect the system dynamics:

Assumption 2: There exist $\overline{d}_0, \overline{d}_1, \overline{\Delta}_0, \overline{\Delta}_1 \geq 0$ such that

$$\|d(x, u, t)\| \leq \overline{d}_0 + \overline{d}_1\|u\|,$$

$$\|\Delta(x, u, t)\| \leq \overline{\Delta}_0 + \overline{\Delta}_1\|u\|, \qquad (34)$$

$\forall(x, t) \in (\partial\mathcal{S} \times \mathbb{T})$ and $\forall u \in \mathbb{U}$.

Remark 6: While ultimate boundedness ($\overline{d}_1 = \overline{\Delta}_1 = 0$) is a common assumption in the RCBF literature [13], [21], [50], [70], it may be too restrictive when the uncertainty scales with the control input (an example will be given in the next part). We include the terms $\overline{d}_1$ and $\overline{\Delta}_1$ to incorporate an affine relationship between $\|u\|$ and the uncertainty bound. While a similar problem was studied in [32] for $\overline{d}_0 = \overline{\Delta}_0 = \overline{\Delta}_1 = 0$, our solution accounts for a more general problem and requires extra conditions to ensure the feasibility.

We consider a compensation of the form:

$$\sigma_1(x, u, t) = \|L_g h(x, t)\|\left(\overline{d}_0 + \overline{d}_1\|u\|\right)$$
$$+ \|\nabla h(x)\|\left(\overline{\Delta}_0 + \overline{\Delta}_1\|u\|\right). \qquad (35)$$

The set of K_{RCBF} with σ_1 becomes

$$K_{\text{RCBF}}^{\sigma_1}(x, t) = \big\{ u \in \mathbb{U} \mid L_g h(x, t)u$$
$$- \|L_g h(x)\|\left(\overline{d}_0 + \overline{d}_1\|u\|\right) - \|\nabla h(x)\|\overline{\Delta}_1\|u\| \geq -\Psi(x, t) \big\}, \qquad (36)$$

where $\Psi(x, t) \triangleq L_f h(x, t) + \alpha(h(x)) - \|\nabla h(x)\|\overline{\Delta}_0$. The next theorem provides a novel sufficient condition to ensure the feasibility of the robust safety filter with σ_1.

Theorem 4: Let Assumption 1–2 hold with constants $\rho > 0$ and $\overline{d}_0, \overline{d}_1, \overline{\Delta}_0, \overline{\Delta}_1 \geq 0$, and let $\mathbb{U} = \mathbb{R}^m$. A continuously differentiable function h with a regular value of 0 is a RCBF for the system (18) on $(\mathbb{X} \times \mathbb{T})$ with σ_1 given as in (35) if

$$\overline{d}_1 < 1 - \overline{\Delta}_1/\underline{\rho}, \qquad (37)$$

and

$$\Psi(x, t) > 0, \quad \forall(x, t) \in \mathcal{G}, \qquad (38)$$

where $\Psi(x, t) \triangleq L_f h(x, t) + \alpha(h(x)) - \|\nabla h(x)\|\overline{\Delta}_0$. This implies that, should (37)–(38) hold, the set $K_{\text{RCBF}}^{\sigma_1}(x, t)$ is not empty for any $(x, t) \in (\mathbb{X} \times \mathbb{T})$.

Proof: Our goal is to show that (37)–(38) are sufficient for the RCBF definition (26) with $\sigma = \sigma_1$. We consider two cases separately: $(x, t) \in \mathcal{G}$ and $(x, t) \in (\mathbb{X} \times \mathbb{T}) \setminus \mathcal{G}$.

For the first case, we have $L_g h(x, t) = 0$ (cf. (10)), and the condition in the RCBF definition (26) becomes

$$\Psi(x, t) > \|\nabla h(x)\|\overline{\Delta}_1\|u\|. \qquad (39)$$

If $\|\nabla h(x)\|\overline{\Delta}_1 = 0$, then this condition holds trivially for any $u \in \mathbb{R}^m$ since the left hand side is strictly positive $\forall(x, t) \in \mathcal{G}$ per (38). If $\|\nabla h(x)\|\overline{\Delta}_1 > 0$, then (39) becomes

$$\|u\| < \frac{\Psi(x, t)}{\|\nabla h(x)\|\overline{\Delta}_1}. \qquad (40)$$

Since the right hand side is strictly positive, there exists a $\delta > 0$ such that (40) holds for all u satisfying $\|u\| \leq \delta$. Thus, $K_{\text{RCBF}}^{\sigma_1}(x, t)$ is not empty for any $(x, t) \in \mathcal{G}$.

For the second case, $(x, t) \in (\mathbb{X} \times \mathbb{T}) \setminus \mathcal{G}$ implies $L_g h(x, t) \neq 0$. Thus, $\|\nabla h(x)\| > 0$ and (26) becomes

$$L_g h(x, t)u - \|L_g h(x, t)\|\overline{d}_1\|u\| - \|\nabla h(x)\|\overline{\Delta}_1\|u\| >$$
$$\underbrace{-\Psi(x, t) + \|L_g h(x, t)\|\overline{d}_0}_{\chi(x, t)}. \qquad (41)$$

Since $\mathbb{U} = \mathbb{R}^m$, we can choose u such that $L_g h(x, t)u = \|L_g h(x, t)\|\|u\|$ (i.e., the same direction as the vector $L_g h(x, t)$). This selection simplifies (41) to

$$\left(\underbrace{\|L_g h(x, t)\|(1 - \overline{d}_1) - \|\nabla h(x)\|\overline{\Delta}_1}_{M(x, t)} \right) \|u\| > \chi(x, t). \qquad (42)$$

If $M(x, t) > 0$, then $\exists u \in \mathbb{R}^m$ satisfying (42) regardless of the sign of χ. Thus, $M(x, t) > 0$ is a sufficient condition for the RCBF definition when $(x, t) \in (\mathbb{X} \times \mathbb{T}) \setminus \mathcal{G}$. Recall that $\|\nabla h(x)\| > 0$, which implies $\frac{M(x, t)}{\|\nabla h(x)\|} > 0$ where

$$\frac{M(x, t)}{\|\nabla h(x)\|} = \frac{\|\nabla h(x)^\top g(x, t)\|}{\|\nabla h(x)\|}(1 - \overline{d}_1) - \overline{\Delta}_1. \qquad (43)$$

Here we used $L_g h(x, t) = \nabla h(x)^\top g(x, t)$. Note that $1 - \overline{d}_1 > 0$ per (37). Since (31) implies

$$\min_{q \in \mathbb{R}^m \setminus \{0\}} \frac{\|q^\top g(x, t)\|}{\|q\|} \geq \underline{\rho}, \quad \forall(x, t) \in (\mathbb{X} \times \mathbb{T}), \qquad (44)$$

we have

$$\frac{M(x, t)}{\|\nabla h(x)\|} \geq \underline{\rho}(1 - \overline{d}_1) - \overline{\Delta}_1. \qquad (45)$$

Using (37) we can show that $\frac{M(x, t)}{\|\nabla h(x)\|} > 0$. Thus, (37)–(38) are sufficient for the RCBF condition (26) with σ_1. $\blacksquare$

Theorem 4 provides a condition for the existence of a controller ensuring robust safety when $\mathbb{U} = \mathbb{R}^m$. While it is typically a challenging problem to find such explicit conditions for $\mathbb{U} \subset \mathbb{R}^m$, recent developments led to a rigorous framework for incorporating input bounds implicitly using backup CBFs [71], even for a robust problem [72].

Remark 7: If we consider the case $\overline{\Delta}_1 = 0$, then the sufficient condition (37) simplifies to $\overline{d}_1 < 1$, which is equivalent to the condition found in [32] (given as $0 \leq \overline{d} < 1$). However, with $\overline{\Delta}_1$, the condition (37) includes the case of an unmatched uncertainty changing with u.

Condition (38) implies that when $L_g h(x, t) = 0$ the barrier function condition $\dot{h} \geq -\alpha(h)$ should be attainable merely by f under the worst case scenario. The existence of a $\alpha \in \mathcal{K}_\infty^e$ satisfying (38) with given f and $\overline{\Delta}_0$ is a property that h should have for the RCBF definition.

Theorem 4 provides sufficient conditions ensuring the point-wise feasibility of the robust safety filter with the compensation σ_1, which is tailored to cancel the uncertainty in a worst-case manner.

Theorem 5: Let Assumption 1–2 hold with constants $\rho > 0$ and $\overline{d}_0, \overline{d}_1, \overline{\Delta}_0, \overline{\Delta}_1 \geq 0$. If h is a RCBF for the system (18) with σ_1 as in (35), then the system (19) is safe w.r.t. $\mathcal{S}$ when $u = k_{\text{OP}}(x, t)$ if k_{OP} is locally Lipschitz continuous in x and piecewise continuous in t.

Proof: Considering Assumption 1 and the compensation σ_1 as in (35), the condition (28) becomes:

$$L_g h(x, t) d(x, u, t) + \nabla h(x)^\top \Delta(x, u, t)$$
$$+ \|L_g h(x, t)\| \left(\overline{d}_0 + \overline{d}_1 \|u\| \right) + \|\nabla h(x)\| \left(\overline{\Delta}_0 + \overline{\Delta}_1 \|u\| \right) \geq 0. \tag{46}$$

Thus, if the uncertainty satisfies Assumption 2 with constants $\overline{d}_0, \overline{d}_1, \overline{\Delta}_0, \overline{\Delta}_1 \geq 0$, the compensation σ_1 as in (35) satisfies the condition (28). Theorem 3 completes the proof. ∎

It is noted that the safety constraint becomes non-smooth due to $\|u\|$, therefore duality conditions cannot be used to calculate the closed-form solution in a general case. Yet, it can be shown that the constraints in the OP (29) can be represented as a rotated second order cone, and thus can be solved effectively using efficient algorithms such as [73]. Moreover, a closed-form solution may exist for the scalar input case.

Remark 8: The lack of a general solution prevents us showing the Lipschitz continuity for the robust safety filter with σ_1. In [52], authors show that relaxing the safety constraint with a slack variable can ensure Lipschitz property at the expense of losing the safety guarantee. Furthermore, authors in [32] 'conjecture that the solution remains locally Lipschitz continuous when the constraint is described by two second order cone constraints'. Showing the Lipschitz properties for a general case is left for a future work. The scalar input case has the same Lipschitz properties as the QP in (16).

B. EXAMPLE

To demonstrate the theoretical concepts we consider a pendulum, depicted in Fig. 1, whose angle from the vertical position denoted as θ. A mass m is carried by the massless rod and its distance from the pivot l changes periodically in time according to a time-dependent constraint. A motor provides the control torque u and G is the gravitational acceleration. This may be considered as the simplest model for a child on a swing who is moving its center of mass up and down to
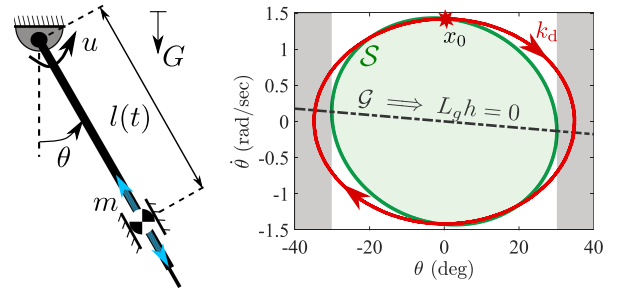

FIGURE 1. (Left panel) Mechanical model of a swing. The distance *l* changes periodically. (Right panel) The safety goal $\theta \leq \theta_{\text{max}}$ as the white rectangle, the set $\mathcal{S}$ as green ellipse, the set $\mathcal{G}$ highlighted by the dashed-dotted line, and the simulated trajectory for $u = k_d(x, t) \equiv 0$ is shown by the red curve.

destabilize the hanging down position while the input torque is applied to ensure safe swinging.

The equation of motion is derived in Appendix A using Lagrangian equations. Choosing the angle and angular speed as states, i.e., $x \triangleq [\theta, \dot{\theta}]^\top$, we can obtain:

$$\dot{x} = \underbrace{\begin{bmatrix} x_2 \\ -\frac{G}{l(t)} \sin x_1 - 2\frac{\dot{l}(t)}{l(t)} x_2 \end{bmatrix}}_{f(x,t)} + \underbrace{\begin{bmatrix} 0 \\ \frac{1}{ml(t)^2} \end{bmatrix}}_{g(t)} u. \tag{47}$$

It is noted that the system functions f and g can be calculated explicitly when $l(t)$ and $\dot{l}(t)$ are given. We let $\mathbb{U} = \mathbb{R}$.

To enforce physical safety, we want to limit the angle: $|\theta| \leq \theta_{\text{max}} = \pi/6$. Excluding $\dot{\theta}$ from $h(x)$ would imply that $\mathcal{G} = \mathbb{R}^2 \times \mathbb{R}$, and the necessary condition (11) cannot be shown for a general periodic excitation of $l(t)$. Thus, we enforce the goal using a quadratic function $h : \mathbb{R}^2 \to \mathbb{R}$:

$$h(x) = \frac{1}{2} x^\top A x + c, \quad A = \begin{bmatrix} a_1, a_2 \\ a_2, a_3 \end{bmatrix}, \quad \begin{array}{l} A \text{ is negative definite,} \\ a_2 < 0, \quad c > 0. \end{array} \tag{48}$$

The corresponding set $\mathcal{S} \in \mathbb{R}^2$ is an ellipse with a slight tilt in counterclockwise direction for $a_2 < 0$, see the green domain in Fig. 1 for parameters $a_1 = -7.30$, $a_2 = -0.25$ s, $a_3 = -1$ s^2 and $c = 1$. Observe that $\mathcal{S}$ is a subset of the original safety goal $|\theta| \leq \theta_{\text{max}}$ (white region). Therefore, ensuring the invariance of $\mathcal{S}$ is sufficient. We take the desired controller as $k_d(x, t) \equiv 0$, and simulate (47) for $m = 30$ kg and $l(t) \equiv L = 1.75$ m (this time-invariant configuration is denoted as case (A)). Starting from $x_0 = [0, 1.4 \,\text{rad/s}]^\top$, the simulated trajectory (red curve in Fig. 1) leaves $\mathcal{S}$ even for a constant l. Below we design safety filters to ensure safety w.r.t. $\mathcal{S}$ for two scenarios: ideal and partially known models.

1) IDEAL CASE

We will use safety filter to keep the system safe. To do this, first we need to show that h is a CBF for the system (48).

Proposition 1: The function h as defined in (48) is a CBF for (47) with $\alpha(h) = \alpha_c h$ for any $\alpha_c > 0$.

The proof of Proposition 1 is given in Appendix B. Since $\mathbb{U} = \mathbb{R}$ and $m = 1$, the closed form solution of the safety
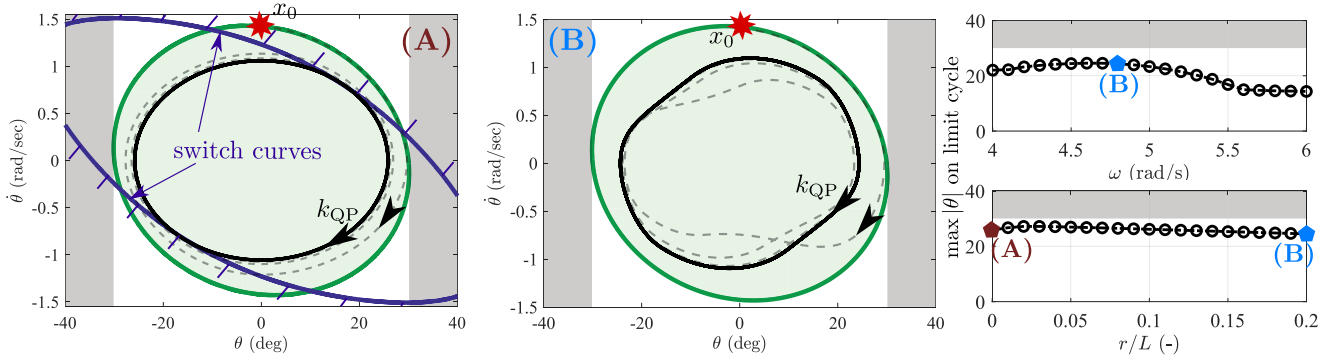
FIGURE 2. (Left panel) Simulated trajectories when the safety filter is implemented for case (A), and curves marking where the desired controller is intervened. (Middle panel) Simulated trajectory when the safety filter is implemented for case (B). (Right panel) The maximum θ along the limit cycle as a function of ω (for $r/L = 0.2$) and r/L (for $\omega = 4.8$ rad/s).

filter in (16) can be implemented. The system is simulated with the same conditions as above (case (A) and same x_0) using $\alpha_c = 1.5$ 1/s, see the black trajectory in the left panel of Fig. 2. When θ approaches $\theta_{\max}$ with a large rate $\dot{\theta}$, the safe control is activated, i.e., $k_{QP}(x, t) = \Phi_{QP}(x, t)$, and it slows down the swing to ensure safety. The controller switches back to $k_d(x, t) = 0$ when state is ensured to be contained in $\mathcal{S}$ with no control. This cycle is repeated until the trajectory converges to a stable limit cycle inside $\mathcal{S}$.

The curve where the switch occurs between safe control and no control can be found explicitly using $\Phi_{QP}(x, t) = k_d(x, t) = 0$. This equation yields two solutions in the form of time-varying parabolas in the state space (depicted in the left panel of Fig. 2 for case (A)). We have $k_{QP}(x, t) \equiv k_d(x, t)$ inside the curves, and $k_{QP}(x, t) = \Phi_{QP}(x, t)$ outside. Note that the stable limit cycle that trajectories converge to *grazes* the switch curves, which implies that its shape can be modified through h and α. We leave the further analysis of the effect of these particular selections on the nonlinear characteristics of the system trajectories as a future work, and focus on improving the resilience of the CBF condition against uncertainties.

Next, we consider the case where a periodic excitation of the form $l(t) = L + r\sin(\omega t)$ is introduced with *known* amplitude and frequency values (case (B) is for $r/L = 0.2$ and $\omega = 4.8$ rad/s). Implementing the safety filter (16) successfully keeps the system safe, because it has full information of the model $f(x, t)$ and $g(t)$, see the middle panel of Fig. 2. The safety results hold for different ω and r values. The right panel in Fig. 2 shows the values $\max |\theta(t)|$ over all $t > t_s$, where t_s denotes the time it takes for trajectories to converge to the limit cycle.

2) PARTIALLY KNOWN MODEL

Let us consider the case where the amplitude of the periodic excitation, r, is not known. The uncertainty emerging from the unknown periodic excitation can be separated from the known part in (47) (called the 'nominal system'). We give detailed calculations in Appendix C, where we use Taylor expansion
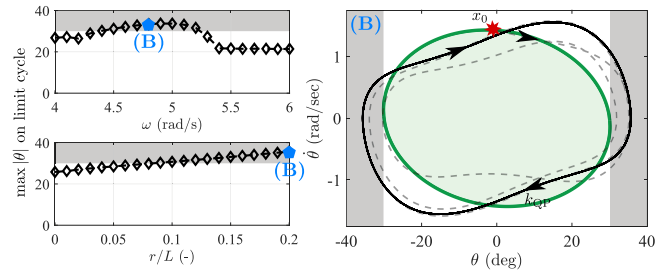

FIGURE 3. Simulation results when the safety filter k_{QP} is implemented with partial information. (Left panel) The maximum θ along the limit cycle as a function of ω (for $r/L = 0.2$), and r/L (for $\omega = 4.8$ rad/s). (Right panel) Simulated trajectory for case (B).

with the assumption $r \ll L$ to obtain:

$$\dot{x} = \underbrace{\begin{bmatrix} x_2 \\ -\frac{G}{L}\sin x_1 \end{bmatrix}}_{f(x)} + \underbrace{\begin{bmatrix} 0 \\ \frac{1}{mL^2} \end{bmatrix}}_{g} u$$
$$+ \underbrace{\begin{bmatrix} 0 \\ \frac{r}{L}\left(\frac{G}{L}\sin(\omega t)\sin x_1 - 2\omega\cos(\omega t)x_2 - \frac{2}{mL^2}\sin(\omega t)u\right) \end{bmatrix}}_{\mu(x,u,t)},$$
$$(49)$$

cf. (47). The function μ represents the uncertainty, and it depends on state, input, and time. When we design the safety filter (16) considering $\mu \equiv 0$, the resulting controller becomes indifferent to the periodic excitation. Consequently, we observe $\theta > \theta_{\max}$ for a large enough r at certain ω, see the left panel in Fig. 3. The visual depiction of the safety violation is given in the right panel for case (B).

Our goal is to design a robust safety filter using σ_1 as in (35). To use this framework we check Assumption 1–2. Assumption 1 is satisfied for (49) since $g \neq 0$. In addition, in Appendix C we show that

$$\Delta(x, u, t) \equiv 0 \quad \Rightarrow \quad \overline{\Delta}_0 = \overline{\Delta}_1 = 0, \qquad (50)$$
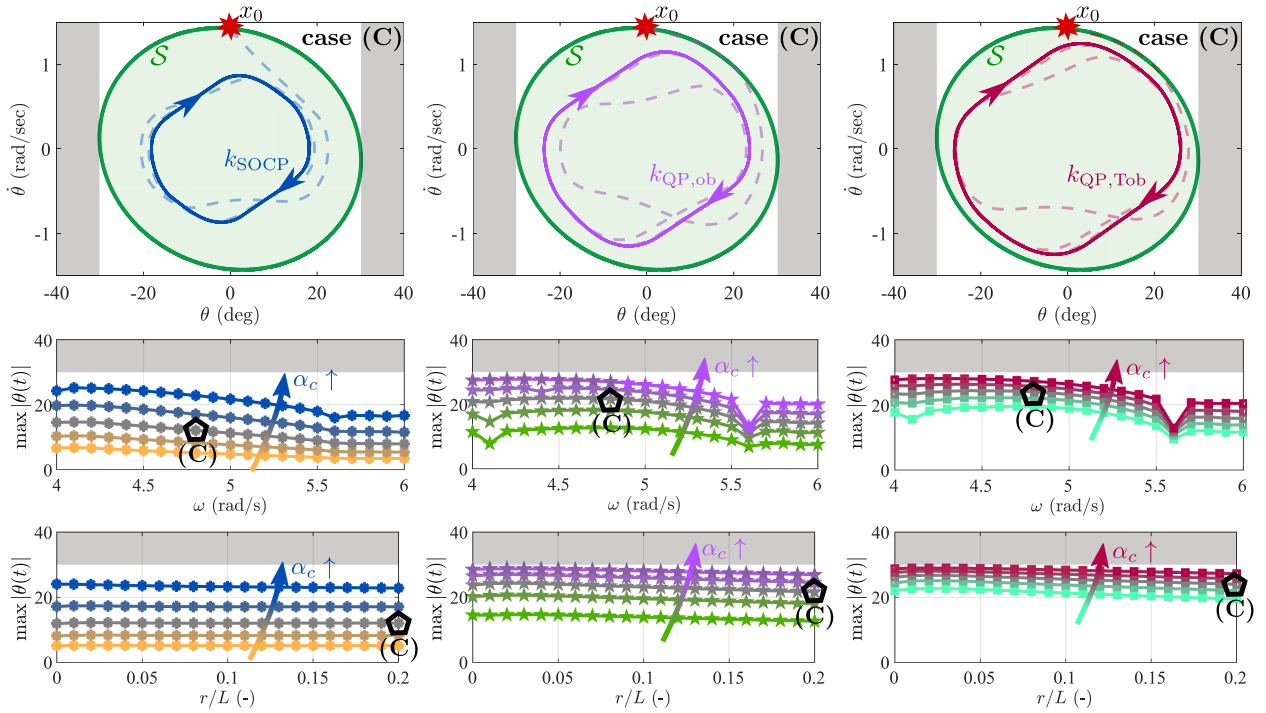
FIGURE 4. Left, middle and right panels show simulation results for the robust safety filters with σ_1, σ_2 and σ_3, respectively. The top row depicts the trajectories for the case (B). The bottom two rows demonstrate the robust safety results for various *unknown* periodic excitation $r \leq \bar{r}$ and $\omega \leq \bar{\omega}$. Increasing α_c allows trajectories to get closer to the boundary of $\mathcal{S}$.

$$d(x, u, t) \leq \overline{d}_0 + \overline{d}_0 |u|, \tag{51}$$

cf. (34), and that assuming $r \leq \overline{r}$ and $\omega \leq \overline{\omega}$ we have

$$\overline{d}_0 \approx 2mL\overline{r\omega}\sqrt{\frac{2c}{-a_3}}, \qquad \overline{d}_1 = 2\frac{\overline{r}}{L}. \tag{52}$$

We pick $\overline{r} = 0.2L$ and $\overline{\omega} = 6.0$ rad/s, which yields $\overline{d}_0 = 310$ Nm and $\overline{d}_1 = 0.4$.

With Assumption 1–2 satisfied, we can utilize σ_1 as in (35) for robust safety. Note that the condition (37) holds since $\overline{\Delta}_1 = 0$ and $\overline{d}_1 < 1$. Moreover, since $\overline{\Delta}_0 = 0$, (38) simplifies to $L_f h(x, t) + \alpha(h(x)) > 0$, cf. (36). This condition holds since h was shown to be a CBF for (47), see Remark 3. Consequently, Theorem 4 establishes that h is a RCBF.

Proposition 2: The function h in (48) is a RCBF for (49) with $\alpha(h) = \alpha_c h$ and σ_1 as in (35) for any $\alpha_c > 0$.

The robust safety filter with σ_1 will be called as k_{SOCP}. Implementing k_{SOCP} for different values of $\alpha_c \in [0.75, 7.5]$ 1/s, $r \leq \overline{r}$ and $\omega \leq \overline{\omega}$, we give simulation results in the left panels of Fig. 4. The trajectory for $\alpha_c = 1.5$ 1/s (case C) is depicted in the top panel, which converges to a limit cycle inside $\mathcal{S}$ without leaving it. We find the values max $|\theta(t)|$ over all $t > t_s$, where t_s denotes the settling time of convergence to the limit cycle. Our findings, shown in the bottom two panels, align with the theoretical results.

IV. LESS CONSERVATIVE CONTROLLER DESIGN

This section presents more sophisticated methodologies to design less conservative robust safety-critical controllers,

leveraging observer-based uncertainty estimation and tunable compensatory mechanisms to improve control performance while maintaining rigorous safety guarantees.

A. OBSERVER-BASED CONTROLLER

Recall that, with the uncertainty μ, $\dot{h}$ becomes:

$$\dot{h}(x, u, t) = L_f h(x, t) + L_g h(x, t)u + L_\mu h(x, u, t). \tag{53}$$

While the function $L_\mu h$ is unknown, it can be *estimated* so that the barrier function-based safety condition $\dot{h} \geq -\alpha(h)$ can be ensured less conservatively.

Assumption 3: Given a controller $k : \mathbb{X} \times \mathbb{T} \to \mathbb{U}$, there exist functions $\widehat{L_\mu h} : \mathbb{X} \times \mathbb{T} \to \mathbb{R}$ and $\Gamma : \mathbb{T} \to \mathbb{R}$ such that:

$$\left| L_\mu h\left(x(t), k(x(t), t), t\right) - \widehat{L_\mu h}(x(t), t) \right| \leq \Gamma(t), \quad \forall t \geq t_0. \tag{54}$$

This assumption implies the existence of an estimator with a deterministic error bound. Some of the well-known observer and estimator techniques were implemented in the CBF framework to satisfy Assumption 3, for example, [29], [36], [37], [38], [39], [40], [41]. In an effort of finding an estimator satisfying Assumption 3, we propose the function $\sigma_2 : \mathbb{X} \times \mathbb{T} \to \mathbb{R}$:

$$\sigma_2(x, t) = -\widehat{L_\mu h}(x, t) + \Gamma(t), \tag{55}$$

where the first term cancels $L_\mu h$, and the second term compensates for the residual error.

Assumption 4: The input relative degree of h is less than or equal to the uncertainty relative degree of h:

$$L_\mu h(x, u, t) = 0, \qquad \forall(x, t) \in \mathcal{G}, \ \forall u \in \mathbb{U}. \quad (56)$$

This assumption implies that the lowest-order time derivative of h that the uncertainty μ can affect is equal to or higher than the lowest-order time derivative of h that the input u can affect. Consequently, the term $L_\mu h$ can be canceled in $\dot{h}$ using u. Assumption 4, which can be relaxed, see Remark 10, allows us to find sufficient conditions such that h is a RCBF. In particular, using (56), the bound (54) implies

$$\widehat{L_\mu h}(x(t), t) \geq -\Gamma(t), \ \forall(x, t) \in \mathcal{G}. \quad (57)$$

Thus, extending Remark 3 for the RCBF definition requires

$$L_f h(x, t) \geq -\alpha(h(x)) + 2\Gamma(t), \ \forall(x, t) \in \mathcal{G}, \quad (58)$$

to hold for the inequality (26). If $\mathbb{U} = \mathbb{R}^m$, (58) is a necessary and sufficient condition for (26).

Theorem 6: Let $\mathcal{S}$ be the 0-superlevel set defined as in (3) with a continuously differentiable function $h : \mathbb{X} \to \mathbb{R}$, and let 0 be a regular value of h. Let the uncertainty μ and functions $\widehat{L_\mu h}$ and Γ satisfy Assumptions 3 and 4.
- If $\mathbb{U} = \mathbb{R}^m$, then h is a RCBF for (18) on $(\mathbb{X} \times \mathbb{T})$ with σ_2 in (55) if and only if (58) holds.
- If h is a RCBF for (18) on $(\mathbb{X} \times \mathbb{T})$ with σ_2, then the system (19) is safe w.r.t. $\mathcal{S}$ when $u = k_{\text{OP}}(x, t)$.
- Substituting σ_2, the OP in (29) becomes a QP. Furthermore, if $\mathbb{U} = \mathbb{R}^m$, then the QP has a closed-form solution given in the form (13)–(14) with $\Phi(x, t) = \Phi_{\text{ob}}(x, t)$ defined as:

$$\Phi_{\text{ob}}(x, t) \triangleq -\frac{L_f h(x, t) + L_g h(x, t) k_{\text{d}}(x, t) + \alpha(h(x)) - \sigma_2(x, t)}{\|L_g h(x, t)\|^2}. \quad (59)$$

Proof: The proof for the first two statements can be extended from the discussion in Remark 3 and the proof of Theorem 5, respectively. Furthermore, since the OP becomes a QP with σ_2, the last bullet point can be followed from the proof of Theorem 2 (as given in [21], [60], [62]) with simple modifications for σ_2. ∎

Remark 9: Analogous to the CBF-based QP (16), the robust safety filter (13)–(14) with (59) can be simplified for the scalar input case ($m = 1$):

$$k_{\text{QP,ob}}(x, t) = \begin{cases} \min\{k_{\text{d}}(x, t), \Phi_{\text{QP,ob}}(x, t)\} & \text{if } L_g h(x, t) < 0, \\ \max\{k_{\text{d}}(x, t), \Phi_{\text{QP,ob}}(x, t)\} & \text{if } L_g h(x, t) > 0, \\ k_{\text{d}}(x, t) & \text{if } L_g h(x, t) = 0, \end{cases} \quad (60)$$

where $\Phi_{\text{QP,ob}} : \mathbb{X} \times \mathbb{T} \to \mathbb{R}$ is defined as

$$\Phi_{\text{QP,ob}}(x, t) = -\frac{L_f h(x, t) + \alpha(h(x)) + \widehat{L_\mu h}(x, t) - \Gamma(t)}{L_g h(x, t)}. \quad (61)$$

HIGH-GAIN DISTURBANCE OBSERVER

Motivated by the estimator-based compensation setup, we consider an observer $\widehat{L_\mu h} : \mathbb{X} \times \mathbb{T} \to \mathbb{R}$ utilized in [35], [37]:

$$\widehat{L_\mu h}(x(t), t) = k_{\text{obs}} h(x(t)) - \zeta(t), \quad (62)$$

where $k_{\text{obs}} > 0$ is the observer gain and $\zeta(t)$ denotes an auxiliary state. In particular, given an initial condition $\zeta(0) = \zeta_0$, $\zeta(t)$ satisfies the following ODE:

$$\dot{\zeta}(t) =$$

$$k_{\text{obs}} \left(\underbrace{L_f h(x(t), t) + L_g h(x(t), t) u(t) + k_{\text{obs}} h(x(t))}_{\Psi(x(t), u(t), t)} - \zeta(t) \right). \quad (63)$$

Note that (63) is a linear ODE, and convolution integral can be used to find the solution:

$$\zeta(t) = \zeta_0 e^{-k_{\text{obs}} t} + k_{\text{obs}} \int_0^t e^{-k_{\text{obs}}(t - \tilde{t})} \Psi\left(x(\tilde{t}), u(\tilde{t}), \tilde{t}\right) d\tilde{t}. \quad (64)$$

We can find a deterministic error bound $\Gamma(t)$ for the observer (62). Focusing on the explicit time dependency with a slight abuse of notation, we use $L_\mu h(t) = L_\mu h(x(t), u(t), t)$.

Assumption 5: There exist constants $\overline{L_\mu h}_0, \mathcal{L} \geq 0$ such that:

$$\left| L_\mu h(t_0) \right| \leq \overline{L_\mu h}_0, \ \forall t_0 \in \mathbb{R}, \quad (65)$$

$$\left| L_\mu h(r) - L_\mu h(s) \right| \leq \mathcal{L} |r - s|, \ \forall r, s \in \mathbb{T} = [t_0, \infty). \quad (66)$$

While (65) accounts for the boundedness of the initial uncertainty, (66) constitutes an upper bound on how fast the effect of the uncertainty changes in time. That is, $\mathcal{L}$ is the Lipschitz constant of $L_\mu h$ in t. Lipschitz bounds are commonly utilized in RCBF formulations [42], [43], [52] and these can be obtained from sampled data using Strongin's estimator [74], [75].

Using the observer error $e(t) \triangleq L_\mu h(t) - \widehat{L_\mu h}(t)$, the following lemma gives us the error bound $\Gamma(t)$.

Lemma 3 ([35]): Consider a function h with the time derivative given in (53) and an observer defined in (62)–(64) with a gain $k_{\text{obs}} > 0$ and the initial condition $\zeta_0 = k_{\text{obs}} h(x_0)$. Let the function $L_\mu h$ satisfy Assumption 5. Then, the following bound holds for the observer error $e(t) = L_\mu h(t) - \widehat{L_\mu h}(t)$:

$$|e(t)| \leq \underbrace{\left(\overline{L_\mu h}_0 - \frac{\mathcal{L}}{k_{\text{obs}}} \right) e^{-k_{\text{obs}} t} + \frac{\mathcal{L}}{k_{\text{obs}}}}_{\Gamma(t)}, \quad \forall t \in \mathbb{T}. \quad (67)$$

The proof (which can be seen in [35] in detail) is omitted here. Starting from $|e(t_0)| = \overline{L_\mu h}_0$, the error moves into a narrower band determined by $\frac{\mathcal{L}}{k_{\text{obs}}}$ as the time progresses (assuming $\overline{L_\mu h}_0 > \frac{\mathcal{L}}{k_{\text{obs}}}$). Note that the faster the uncertainty

dynamics are (specified by a larger $\mathcal{L}$), the wider the steady-state error band gets. A larger k_{obs} not only shrinks the steady state error band, but it also forces a faster initial decay.

Lemma 3 implies that the observer (62) and the error bound (67) satisfy Assumption 3. Under Assumption 4, see Remark 10, Theorem 6 can be used to obtain safety results for the observer-based robust safety filter. We note that, for the observer (62), the necessary condition (58) becomes:

$$L_f h(x, t) \geq -\alpha(h(x)) + 2 \max \left\{ \overline{L_\mu h}_0, \frac{\mathcal{L}}{k_{\text{obs}}} \right\},$$
$$\forall (x, t) \in \mathcal{G}. \tag{68}$$

More accurate initial uncertainty guess and smaller rate of change of the uncertainty can alleviate the condition (68).

Remark 10: Assumption 4 can be relaxed for the observer scheme discussed here. Details can be obtained in references [36], [68], yet, in short, the observer can be extended to estimate disturbances on $\dot{x}$ rather than $\dot{h}$. Then, a high relative degree CBF framework [8], [9] can be used to ensure robust safety in the case the input relative degree is more than the uncertainty relative degree.

Remark 11: There is a causality issue hidden when the observer (62) is implemented to a control system (18), and at the same time the observed value $\widehat{L_\mu h}$ is used to calculate a control input u. In particular, calculating the controller $u(t)$ using (59) requires $\zeta(t)$ (plug (62) into (55)). Yet, (64) implies that ζ depends on the function $u(\tilde{t})$ over $\tilde{t} \in [t_0, t]$. We break this causality loop in the implementation by using a delayed input when calculating (64) (single time interval). Investigating the effect of this ad-hoc solution in a mathematically rigorous way using control barrier functionals [76] is left as future work. We note that we observed this effect to be negligible in our examples.

B. TUNABILITY-BASED CONTROLLER

The difference between an oracle safety filter (with full model information) and a robust design emerges from two sources: the uncertainty in the model $L_\mu h$, and the term σ used to compensate for it, cf. (8) and (26). The observer (62) alleviates both as the observer gain k_{obs} increases. Indeed, for $k_{\text{obs}} \to \infty$, we get $\widehat{L_\mu h} \to L_\mu h$ and $\Gamma \to 0$. However, in practice, a high observer gain k_{obs} makes the closed-loop system more susceptible to imperfections, e.g., the system may become unstable in the presence of input delay [35].

Even for a limited observer gain it is still possible to decrease the difference between the oracle design and a robust safety filter with observer. To see this, notice that the sufficient condition (28) for robust safety is defined on $x \in \partial \mathcal{S}$. Thus, Γ can be reshaped inside $\mathcal{S}$ as long as it satisfies (28) on the boundary. Motivated by this observation, as is done in the tunable ISSf case in (25), the compensation can be reduced based on how far away a state is from the boundary of $\mathcal{S}$ [18]. In particular, we propose

$$\sigma_3(x, t) = -\widehat{L_\mu h}(x, t) + \Gamma(t) \epsilon(h(x)), \tag{69}$$

where, the function $\epsilon : \mathbb{R} \to \mathbb{R}$ satisfies

$$\epsilon(r) \geq 0, \quad \forall r \in \mathbb{R}, \text{ and } (1 - \epsilon) \in \mathcal{K}^{\text{e}}. \tag{70}$$

The second condition in (70) implies that $\epsilon(0) = 1$, thus (28) holds for σ_3 with an observer satisfying Assumption 3 since $x \in \partial \mathcal{S} \Rightarrow h(x) = 0 \Rightarrow \sigma_3(x, t) \equiv \sigma_2(x, t)$. The class-$\mathcal{K}$ property of $1 - \epsilon$ implies $\epsilon(h(x)) < 1$ if $h(x) > 0$. Therefore, the effect of the error compensation term in (69) gets mitigated inside $\mathcal{S}$. As a result, the *tunability* modification yields less conservative robust safety filters.

Remark 12: Even the necessary condition for the RCBF definition is relaxed with ϵ, cf. (58):

$$L_f h(x, t) \geq -\alpha(h(x)) + 2\Gamma(t)\epsilon(h(x)),$$
$$\forall (x, t) \in \mathcal{G} \cap (\mathbb{X} \times \mathbb{T}). \tag{71}$$

Theorem 7: Let $\mathcal{S}$ be the 0-superlevel set defined as in (3) with a continuously differentiable function $h : \mathbb{X} \to \mathbb{R}$, and let 0 be a regular value of h. Let the uncertainty μ and functions $\widehat{L_\mu h}$ and Γ satisfy Assumptions 3 and 4. Let ϵ satisfy (70).
- If $\mathbb{U} = \mathbb{R}^m$, then h is a RCBF for (18) on $(\mathbb{X} \times \mathbb{T})$ with σ_3 in (69) if and only if (71) holds.
- If h is a RCBF for (18) on $(\mathbb{X} \times \mathbb{T})$ with σ_3, then the system (19) is safe w.r.t. $\mathcal{S}$ when $u = k_{\text{OP}}(x, t)$.
- Substituting σ_3, the OP in (29) becomes a QP. Furthermore, if $\mathbb{U} = \mathbb{R}^m$, then the QP has a closed-form solution given in the form (13)–(14) with $\Phi(x, t) = \Phi_{\text{Tob}}(x, t)$ defined as:

$$\Phi_{\text{Tob}}(x, t) \triangleq -\frac{L_f h(x, t) + L_g h(x, t) k_{\text{d}}(x, t) + \alpha(h(x)) - \sigma_3(x, t)}{\|L_g h(x, t)\|^2}. \tag{72}$$

Proof: The proof of Theorem 6 can be followed with the only change ϵ. ∎

Remark 13: If the function ϵ is continuously differentiable on a closed interval, then it is Lipschitz continuous. As a result, the Lipschitz properties of the resulting controller is the same as the observer-based QP.

Remark 14: Similar to the observer-based method, the robust safety filter (13)–(14) with (72) simplifies for scalar input:

$$k_{\text{QP,Tob}}(x, t) = \begin{cases} \min\{k_{\text{d}}(x, t), \Phi_{\text{QP,Tob}}(x, t)\} & \text{if } L_g h(x, t) < 0, \\ \max\{k_{\text{d}}(x, t), \Phi_{\text{QP,Tob}}(x, t)\} & \text{if } L_g h(x, t) > 0, \\ k_{\text{d}}(x, t) & \text{if } L_g h(x, t) = 0, \end{cases} \tag{73}$$

where

$$\Phi_{\text{QP,Tob}}(x, t) = -\frac{L_f h(x, t) + \alpha(h(x) + \widehat{L_\mu h}(x, t) - \Gamma(t)\epsilon(h(x)))}{L_g h(x, t)}. \tag{74}$$

Henceforth, we will use an exponential function as ϵ:

$$\epsilon(h(x)) = e^{-\lambda h(x)}, \tag{75}$$

which satisfies (70) for any $\lambda > 0$. Note that $\lambda = 0$ returns to the observer-based design with σ_2 as in (55).

V. EXAMPLE

In this section we continue implementing robust safety filters to the swing example introduced in Section III-B. In particular, we first demonstrate that theoretical findings are supported by numerical simulations for σ_2 and σ_3. Then, the likeness of robust controllers (also including σ_1) to the oracle design is investigated using a performance metric.

A. ROBUST SAFETY FOR PARTIALLY KNOWN MODEL

1) OBSERVER-BASED CONTROLLER

The uncertainty for the swing example is matched, that is, $\Delta(x, u, t) \equiv 0$. Thus, Assumption 4 is trivially satisfied. We use Strongin's estimator [74] with the simulation data from the previous configuration to obtain the Lipschitz constant $\mathcal{L} \approx 8$ 1/s². For simplicity, we assume we have an accurate estimate of the initial error, thus, we use $\overline{L_\mu h}_0 = 0$.

Proposition 3: The function h defined in (48) is a RCBF for (49) with $\alpha(h) = \alpha_c h$ and σ_2 as in (55) with observer (62) for $\alpha_c \geq 2a_2/a_3$ and $k_{obs} > \mathcal{L}a_3/a_2$. This implies that the system (49) is safe w.r.t. $\mathcal{S}$ when $u = k_{QP,ob}(x, t)$ in (60).

Here, $\alpha_c \geq 2a_2/a_3$ and $k_{obs} > \mathcal{L}a_3/a_2$ are imposed to accommodate for the extra term $2\mathcal{L}/k_{obs}$ emerging from (71). Implementing $k_{QP,ob}$, we run simulations using same conditions as the previous case, see the middle panels of Fig. 4. The top panel depicts the robust safety of a single trajectory converging to a limit cycle for case (C). The bottom two panels show $\max |\theta(t)|$ for $k_{obs} = 20$ 1/s $> \mathcal{L}a_3/a_2$ and $\alpha_c \in [0.75, 7.5]$ 1/s $\geq 2a_2/a_3$. Robust safety is consistent.

2) TUNABILITY-BASED CONTROLLER

Next, we consider the observer-based QP enhanced with the tunability feature with ϵ chosen in (75).

Proposition 4: The function h defined in (48) is a RCBF for (49) with $\alpha(h) = \alpha_c h$ and σ_3 as given in (69) with observer (62) and ϵ in (75) for $\alpha_c \geq 2a_2/a_3$, $k_{obs} > \mathcal{L}a_3/a_2$ and $\lambda > 0$. This implies that the system (49) is safe w.r.t. $\mathcal{S}$ when $u = k_{QP,Tob}(x, t)$.

Simulations are repeated for $k_{obs} = 20 > \mathcal{L}a_3/a_2$ 1/s, $\lambda = 5$, and $\alpha_c \in [0.75, 7.5]$ 1/s $\geq 2a_2/a_3$, see the right panel of Fig. 4. Again, the robust safety results are consistent through all simulations.

B. ON THE LIKENESS TO THE ORACLE DESIGN

While increasing α_c yields less restrictive conditions for all configurations, see Fig. 4, it comes with the price of *larger control inputs*. This is especially the case for the SOCP, which requires a more aggressive lower bound for $\dot{h}$ in order to achieve comparable performance. This is demonstrated in Fig. 5, where simulated trajectories are depicted for controllers k_{SOCP} ($\alpha_c = 12$ 1/s) and $k_{QP,Tob}$ ($\alpha_c = 2$ 1/s, $k_{obs} = 20$ 1/s, $\lambda = 5$) with color blue and red, respectively. We also plot the case where an oracle-based safety filter is implemented (i.e., the full model is used) with $\alpha_c = 1.5$ 1/s. Notice that trajectories are very close to each other. Yet, maintaining the motion requires larger control input for the SOCP due to
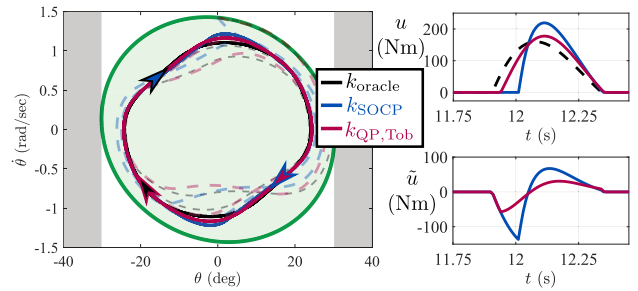

FIGURE 5. Simulated trajectories (left) and control input (right) when the two robust compensation methods as well as the oracle controller (with full model information) are implemented. Although results are very close in the state space, control inputs are considerably different.

its worst-case type of compensation, see the right panel of Fig. 5. The input of the tunability-based case, however, is closer to the oracle thanks to its ability to reject the effect of the unknown dynamics in the controller using $\widehat{L_\mu h}$. The difference between the robust controllers and the oracle is given in the bottom right panel.

Motivated by these observations, we use a performance metric to compare robust controllers. The performance goal for this comparison study is taken as *minimizing the deviation from the oracle controller*. The logic behind this choice is as follows: if we have the perfect information of a system model, then it may be possible to design a controller minimizing a cost function. Comparing robust controllers to this oracle controller serves as a meaningful and practical comparison metric because it eliminates the necessity of specifying this cost. This metric is merely used for comparing these robust controller design principles and it does *not* play a specific role in designing these controllers.

The performance goal is quantified as minimizing the cost $\|k_s(x, t) - k_{oracle}(x, t)\|$, where k_{oracle} denotes the oracle controller that is designed utilizing the ideal model information, and the index s refers to different robust safety filter designs, i.e., SOCP, QP, ob and QP, Tob. In this comparative study, the oracle is represented with data generated using simulations for random system configurations (initial conditions $t_0 \in \mathbb{R}$ and $x_0 \in \mathcal{S}$, and amplitude $r \leq \bar{r}$ and frequency $\omega \leq \overline{\omega}$ of periodic excitation). Overall, we generate $M = 1000$ episodic runs of length N when $u = k_{oracle}(x, t)$ is utilized. We collect the state, time and input data from these runs: x_k^i, t_k^i and u_k^i, where k denotes a time instant in an episode $k = \{1, \ldots, N\}$, and i denotes the number among all episodic runs $i = \{1, \ldots, M\}$. Based on this, we can define the cost:

$$J_s(p) = \frac{1}{MN} \sum_{i=1}^{M} \sum_{k=1}^{N} \left| \underbrace{k_s(x_k^i, t_k^i; p) - u_k^i}_{\tilde{u}_k^i} \right|. \quad (76)$$

to represent the average of the deviation in control $\tilde{u}_k^i$ along trajectories over all episodes. The term p collects the parameters $p = [\alpha_c, k_{obs}, \lambda]^\top$.

We start with the evaluation of k_{SOCP}. The only parameter in this case is α_c. The blue curve in the top panel of Fig. 6
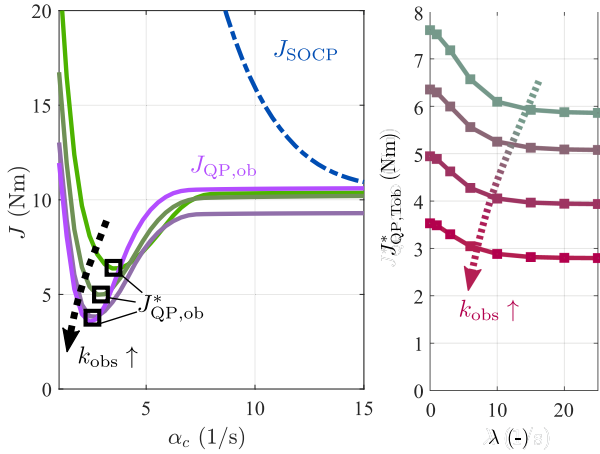
FIGURE 6. (Left) Deviation of the worst-case-based controller from the oracle-based design given by the cost J_{SOCP} as a function of α_c (blue curve), and deviation of the observer-based controller from the oracle-based design given by the cost $J_{QP,ob}$ as a function of α_c for various k_{obs} values (green and purple curves). The minimum values $J^*_{QP,ob}$ decrease as k_{obs} increases. (Right) The minimum values $J^*_{QP,Tob}$ of the cost $J_{QP,Tob}$ over $\alpha_c \in [0.75, 7.5]$ 1/s and $k_{obs} \in \{20, 25, 30, 40\}$ 1/s for a fixed λ. This represents the deviation of the tunable observer-based controller from the oracle-based design as a function λ.

shows that the cost J_{SOCP} decreases monotonously with α_c and it settles around $\sim$10 Nm for large α_c. Next, we evaluate the performance of $k_{QP,ob}$. There are two parameters for this case: α_c and k_{obs}. In particular, k_{obs} increases the rate at which the uncertainty is observed, thus a more accurate cancellation can be obtained in the controller. The cost $J_{QP,ob}$ is depicted in the left panel of Fig. 6 as a function of α_c for $k_{obs} \in \{20, 25, 30, 40\}$ 1/s with different colors. Each curve has a minimum value $J^*_{QP,ob}$, which decreases as k_{obs} is increased. This aligns with the discussion that introducing an estimator mitigates the difference between the robust safety-critical controller and the oracle-based design. Finally, we evaluate the tunability modification $k_{QP,Tob}$ which depends on the parameters α_c, k_{obs} and λ. We compute the cost $J_{QP,Tob}$ and find the minimum $J^*_{QP,Tob}$ over a range of α_c. These minima are depicted in the right panel of Fig. 6 as a function of λ for $k_{obs} \in \{20, 25, 30, 40\}$ 1/s. Note that $\lambda = 0$ means the observer-based design without tunability. Our findings support the argument that tunability (i.e., increasing λ) reduces the deviation from the oracle-based controller.

VI. CONCLUSION

This work investigated the means to obtain robust safety guarantees for control barrier function-based safety-critical controllers in the presence of model uncertainties. We first introduced a general framework providing conditions for robust safety. Then, we utilized the general framework to investigate the robust safety conditions of three design methodologies: a worst-case-based approach, an observer-based approach, and a modification to the latter via tunability. The theoretical results were demonstrated on a practical example of a pendulum with unknown periodic excitation. Finally, we compared the

designs based on a performance metric defined as their deviation from the oracle-based controller. Our findings showed that improved performance could be obtained by introducing means in the controller to estimate the effects of the uncertainty. Further improvements could be shown by reshaping the error compensation based on how safety-critical the state is.

The main future research direction is the development of a broad and systematic framework for merging different robustifying compensation designs to pick the most appropriate design strategy. This framework can include an online scheme to switch between different compensation strategies to adapt dynamically to changing conditions. Moreover, future efforts will be directed to obtain conditions for Lipschitz continuity of RCBF-based controllers.

APPENDIX
A. DERIVING THE EQUATION OF MOTION

We use Lagrange equations of the second kind to derive the equation of motion of the swing example introduced in Section III-B. The degree of freedom of the system is one but the system has a time dependent constraint. Choosing the generalized coordinate θ, the kinetic and potential energy T and U, and virtual power δP of the active force reads:

$$T = \frac{1}{2} m \left(l(t)^2 \dot{\theta}^2 + \dot{l}(t)^2 \right), \tag{77}$$

$$U = -mGl(t)\cos\theta, \tag{78}$$

$$\delta P = u\,\delta\dot{\theta}. \tag{79}$$

The Lagrangian is defined as $L = T - U$ while the last equation gives the generalized force $Q = u$ as the coefficient of the generalized virtual velocity $\delta\dot{\theta}$. The Lagrange equation

$$\frac{\mathrm{d}}{\mathrm{d}t}\frac{\partial L}{\partial \dot{\theta}} - \frac{\partial L}{\partial \theta} = Q, \tag{80}$$

leads to the equation of motion:

$$ml(t)^2\ddot{\theta} + mGl(t)\sin\theta + 2ml(t)\dot{l}(t)\dot{\theta} = u. \tag{81}$$

Choosing the angle and the angular speed as states, i.e., $x \triangleq [\theta, \dot{\theta}]^\top$, we obtain the nonlinear system dynamics:

$$\dot{x} = \underbrace{\begin{bmatrix} x_2 \\ -\frac{G}{l(t)}\sin x_1 - 2\frac{\dot{l}(t)}{l(t)}x_2 \end{bmatrix}}_{f(x,t)} + \underbrace{\begin{bmatrix} 0 \\ \frac{1}{ml(t)^2} \end{bmatrix}}_{g(t)} u. \tag{82}$$

Interested readers can refer to [77], [78] for a detailed nonlinear analysis of a similar system without control.

B. PROOF OF PROPOSITION 1

Proof: We start by showing that 0 is a regular value of h. Since $\nabla h(x) = Ax$, and A is not singular, we have $\nabla h(x) = 0$ only at $x = 0$, which is not in $\partial\mathcal{S}$ for any $c > 0$. Also, note that $\mathcal{S}$ is not empty for any $c > 0$.

Next, we show the necessary and sufficient condition (11) (recall $\mathbb{U} = \mathbb{R}$). We have $a_1, a_2, a_3 < 0$, and $a_1 - a_2^2/a_3 > 0$
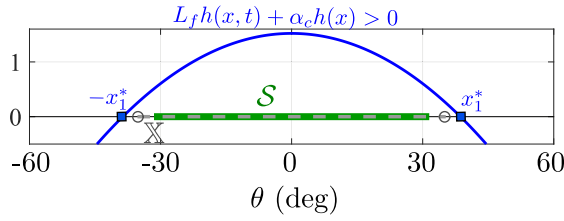
FIGURE 7. The necessary and sufficient condition (11) along the $\mathcal{G}$. One may find a $\mathbb{X} \supset \mathcal{S}$ on which the condition is satisfied.

per the assumptions on A in (48). First, we define the set:

$$\mathcal{G} = \{(x,t) \in (\mathbb{R}^2 \times \mathbb{T}) \mid a_2 x_1 + a_3 x_2 = 0\}, \quad (83)$$

which forms the line $x_2 = -\frac{a_2}{a_3} x_1$ in the state space $\mathbb{R}^2$, see Fig. 1. Choosing $\alpha(h) = \alpha_c h \in \mathcal{K}_\infty^e$ with $\alpha_c > 0$, our goal is to show that there exists an open set $\mathbb{X} \subset \mathbb{R}^2$ such that $L_f h(x,t) + \alpha_c h(x) > 0$ is satisfied $\forall (x,t) \in \mathcal{G}$. Notice that $L_f h(x,t) = -(a_1 - a_2^2/a_3)a_2/a_3 x_1^2$ for all x satisfying $L_g h(x,t) = 0$, thus the condition reduces to

$$\left(a_1 - \frac{a_2^2}{a_3} \right) \left(\frac{\alpha_c}{2} - \frac{a_2}{a_3} \right) x_1^2 + \alpha_c c > 0, \quad (84)$$

which is time-invariant, thus *any* $\mathbb{T} \subset \mathbb{R}$ can be selected.

We separate cases $0 < \alpha_c \leq 2\frac{a_2}{a_3}$ and $\alpha_c > 2\frac{a_2}{a_3}$. For the former, one can show that the coefficient of x_1 becomes non-negative, thus (84) holds over *any* $\mathbb{X} \subset \mathbb{R}^2$. For latter one, the left hand side of (84) becomes a concave parabola that crosses the horizontal axis at

$$x_1 = \pm x_1^* = \pm \sqrt{\frac{-\alpha_c c}{(a_1 - a_2^2/a_3)(\alpha_c/2 - a_2/a_3)}}, \quad (85)$$

see Fig. 7. Notice that $L_f h(x,t) > 0$ for all $(x,t) \in \mathcal{G}$. Thus $L_f h(x,t) + \alpha_c h(x) = 0$ holds if and only if $h(x) < 0$. This implies that $x_1^* \in \mathbb{R}^2 \setminus \mathcal{S}$ regardless of α_c, thus $\mathbb{X}$ can be selected such that $\mathcal{S} \subset \mathbb{X} \subset \mathbb{R}^2$ on which (84) holds. ∎

C. SEPARATING UNCERTAINTY AND FINDING BOUNDS

We use $l(t) = L + r\sin(\omega t)$, yielding $\dot{l}(t) = r\omega\cos(\omega t)$. Considering the amplitude of the periodic excitation as unknown, we can use Taylor expansion to separate the uncertainty from the known portion of the model. In particular, we represent the functions $\frac{1}{l(t)}$, $\frac{\dot{l}(t)}{l(t)}$ and $\frac{1}{l(t)^2}$ using Taylor expansion around $r = 0$. Assuming $r \ll L$ and ignoring the higher order terms yields

$$\frac{1}{l(t)} \approx \frac{1}{L} - \frac{r}{L^2}\sin(\omega t), \quad (86)$$

$$\frac{\dot{l}(t)}{l(t)} \approx \frac{r}{L}\omega\cos(\omega t), \quad (87)$$

$$\frac{1}{l(t)^2} \approx \frac{1}{L^2} - \frac{2r}{L^3}\sin(\omega t). \quad (88)$$

Then, the system dynamics become

$$\dot{x} = \underbrace{\begin{bmatrix} x_2 \\ -\frac{G}{L}\sin x_1 \end{bmatrix}}_{f(x)} + \underbrace{\begin{bmatrix} 0 \\ \frac{1}{mL^2} \end{bmatrix}}_{g} u$$
$$+ \underbrace{\begin{bmatrix} 0 \\ \frac{r}{L}\left(\frac{G}{L}\sin(\omega t)\sin x_1 - 2\omega\cos(\omega t)x_2 - \frac{2}{mL^2}\sin(\omega t)u \right) \end{bmatrix}}_{\mu(x,u,t)}. \quad (89)$$

Finally, we look for bounds on the uncertainty. Using the left pseudo-inverse $g^\dagger = [0 \ mL^2]$ of g, we can separate the uncertainty μ as

$$\Delta(x,u,t) \equiv 0, \quad (90)$$

$$d(x,u,t) = g^\dagger \mu(x,u,t)$$
$$= \frac{r}{L}\left(mGL\sin(\omega t)\sin\theta - 2mL^2\omega\cos(\omega t)\dot{\theta} - 2\sin(\omega t)u \right). \quad (91)$$

Our goal is to look for constants $\overline{d}_0$ and $\overline{d}_1$ such that (34) is satisfied for a reasonable range of periodic excitation $r \leq \overline{r}$ and $\omega \leq \overline{\omega}$. Since $|\sin(\omega t)| \leq 1$ for any ω and t we have

$$\overline{d}_1 = 2\frac{\overline{r}}{L}. \quad (92)$$

Next, we look for the bound $\overline{d}_0$ on $x \in \partial\mathcal{S}$, which is a closed contour of $h(x) = 0$ in $\mathbb{R}^2$, see Fig. 2. The bound $\overline{d}_0$ can be approximated on this contour using $\theta_{\max}$ and $\dot{\theta}_{\max}$, where $\theta_{\max}$ and $\dot{\theta}_{\max}$ denote the maximum values that state variables get on this contour. This leads to

$$\overline{d}_0 = \frac{\overline{r}}{L}\left(mGL\sin\theta_{\max} + 2mL^2\overline{\omega}\dot{\theta}_{\max} \right), \quad (93)$$

cf. (91), where

$$\theta_{\max} = \sqrt{-\frac{2c}{a_1 - a_2^2/a_3}}, \quad \dot{\theta}_{\max} = \sqrt{-\frac{2c}{a_3 - a_2^2/a_1}}. \quad (94)$$

Assuming negligible tilt, that is, $a_2^2 \ll a_1 a_3$, we have $\theta_{\max} \approx \sqrt{\frac{2c}{-a_1}}$ and $\dot{\theta}_{\max} \approx \sqrt{\frac{2c}{-a_3}}$. Furthermore, assuming $\overline{\omega} \gg \frac{G\sin\theta_{\max}}{2L\dot{\theta}_{\max}}$, the second term in d becomes more dominant. Thus, we can get the approximation:

$$\overline{d}_0 \approx 2mL\overline{r}\overline{\omega}\sqrt{\frac{2c}{-a_3}}. \quad (95)$$

REFERENCES
[1] J. Liu, P. Jayakumar, J. L. Stein, and T. Ersal, "A nonlinear model predictive control formulation for obstacle avoidance in high-speed autonomous ground vehicles in unstructured environments," *Veh. Syst. Dyn.*, vol. 56, no. 6, pp. 853–882, 2018.
[2] M. M. Nicotra and E. Garone, "The explicit reference governor: A general framework for the closed-form control of constrained nonlinear systems," *IEEE Control Syst. Mag.*, vol. 38, no. 4, pp. 89–107, Aug. 2018.

[3] S. Bansal, M. Chen, S. Herbert, and C. J. Tomlin, "Hamilton-Jacobi reachability: A brief overview and recent advances," in *Proc. 56th IEEE Conf. Decis. Control*, 2017, pp. 2242–2253.

[4] S. Prajna and A. Jadbabaie, "Safety verification of hybrid systems using barrier certificates," in *Proc. Int. Workshop Hybrid Syst.: Comput. Control.*, 2004, pp. 477–492.

[5] P. Wieland and F. Allgöwer, "Constructive safety using control barrier functions," *IFAC Proc. Volumes*, vol. 40, no. 12, pp. 462–467, 2007.

[6] A. D. Ames, S. Coogan, M. Egerstedt, G. Notomista, K. Sreenath, and P. Tabuada, "Control barrier functions: Theory and applications," in *Proc. Eur. Control Conf.*, 2019, pp. 3420–3431.

[7] X. Xu, J. W. Grizzle, P. Tabuada, and A. D. Ames, "Correctness guarantees for the composition of lane keeping and adaptive cruise control," *IEEE Trans. Automat. Sci. Eng.*, vol. 15, no. 3, pp. 1216–1229, Jul. 2018.

[8] Q. Nguyen and K. Sreenath, "Exponential control barrier functions for enforcing high relative-degree safety-critical constraints," in *Proc. 2016 Amer. Control Conf.*, 2016, pp. 322–328.

[9] W. Xiao and C. Belta, "High-order control barrier functions," *IEEE Trans. Autom. Control*, vol. 67, no. 7, pp. 3655–3662, Jul. 2022.

[10] W. Shaw Cortez, D. Oetomo, C. Manzie, and P. Choong, "Control barrier functions for mechanical systems: Theory and application to robotic grasping," *IEEE Trans. Control Syst. Technol.*, vol. 29, no. 2, pp. 530–545, Mar. 2021.

[11] J. Breeden, K. Garg, and D. Panagou, "Control barrier functions in sampled-data systems," *IEEE Control Syst. Lett.*, vol. 6, pp. 367–372, 2022.

[12] A. K. Kiss, T. G. Molnar, D. Bachrathy, A. D. Ames, and G. Orosz, "Certifying safety for nonlinear time delay systems via safety functionals: A discretization based approach," in *Proc. Amer. Control Conf.*, 2021, pp. 1058–1063.

[13] K. Garg and D. Panagou, "Robust control barrier and control Lyapunov functions with fixed-time convergence guarantees," in *Proc. Amer. Control Conf.*, 2021, pp. 2292–2297.

[14] A. Polyakov and M. Krstic, "Finite- and fixed-time nonovershooting stabilizers and safety filters by homogeneous feedback," *IEEE Trans. Autom. Control*, vol. 68, no. 11, pp. 6434–6449, Nov. 2023.

[15] L. Lindemann and D. V. Dimarogonas, "Control barrier functions for signal temporal logic tasks," *IEEE Control Syst. Lett.*, vol. 3, no. 1, pp. 96–101, Jan. 2019.

[16] S. Kolathaya and A. D. Ames, "Input-to-state safety with control barrier functions," *IEEE Control Syst. Lett.*, vol. 3, no. 1, pp. 108–113, Jan. 2019.

[17] E. D. Sontag, "Smooth stabilization implies coprime factorization," *Trans. Autom. Control*, vol. 34, no. 4, pp. 435–443, Apr. 1989.

[18] A. Alan, A. J. Taylor, C. R. He, G. Orosz, and A. D. Ames, "Safe controller synthesis with tunable input-to-state safe control barrier functions," *IEEE Control Syst. Lett.*, vol. 6, pp. 908–913, 2022.

[19] A. J. Taylor, A. Singletary, Y. Yue, and A. D. Ames, "A control barrier perspective on episodic learning via projection-to-state safety," *IEEE Control Syst. Lett.*, vol. 5, no. 3, pp. 1019–1024, Jul. 2021.

[20] M. Krstic, "Inverse optimal safety filters," *IEEE Trans. Autom. Control*, vol. 69, no. 1, pp. 16–31, Jan. 2024.

[21] M. Jankovic, "Robust control barrier functions for constrained stabilization of nonlinear systems," *Automatica*, vol. 96, pp. 359–367, 2018.

[22] A. Ben-Tal and A. Nemirovski, "Robust solutions of uncertain linear programs," *Operations Res. Lett.*, vol. 25, no. 1, pp. 1–13, 1999.

[23] M. S. Lobo, L. Vandenberghe, S. Boyd, and H. Lebret, "Applications of second-order cone programming," *Linear Algebra Appl.*, vol. 284, no. 1-3, pp. 193–228, 1998.

[24] K. P. Tee, S. S. Ge, and E. H. Tay, "Barrier Lyapunov functions for the control of output-constrained nonlinear systems," *Automatica*, vol. 45, no. 4, pp. 918–927, 2009.

[25] B. T. Lopez, J.-J. E. Slotine, and J. P. How, "Robust adaptive control barrier functions: An adaptive and data-driven approach to safety," *IEEE Control Syst. Lett.*, vol. 5, no. 3, pp. 1031–1036, Jul. 2021.

[26] M. H. Cohen, C. Belta, and R. Tron, "Robust control barrier functions for nonlinear control systems with uncertainty: A duality-based approach," in *Proc. 61st IEEE Conf. Decis. Control*, 2022, pp. 174–179.

[27] T. Pati and S. Z. Yong, "Robust control barrier functions for control affine systems with time-varying parametric uncertainties," *IFAC-PapersOnLine*, vol. 56, no. 2, pp. 10588–10594, 2023.

[28] P. Zhao, Y. Mao, C. Tao, N. Hovakimyan, and X. Wang, "Adaptive robust quadratic programs using control Lyapunov and barrier functions," in *Proc. 59th IEEE Conf. Decis. Control*, 2020, pp. 3353–3358.

[29] Y. Cheng, P. Zhao, and N. Hovakimyan, "Safe and efficient reinforcement learning using disturbance-observer-based control barrier functions," in *Proc. 5th Learn. Dyn. Control Conf.*, 2023, pp. 104–115.

[30] Q. Nguyen and K. Sreenath, "Robust safety-critical control for dynamic robotics," *IEEE Trans. Autom. Control*, vol. 67, no. 3, pp. 1073–1088, Mar. 2022.

[31] T. Wei, S. Kang, W. Zhao, and C. Liu, "Persistently feasible robust safe control by safety index synthesis and convex semi-infinite programming," *IEEE Control Syst. Lett.*, vol. 7, pp. 1213–1218, 2022.

[32] J. Buch, S.-C. Liao, and P. Seiler, "Robust control barrier functions with sector-bounded uncertainties," *IEEE Control Syst. Lett.*, vol. 6, pp. 1994–1999, 2022.

[33] Y. Emam, P. Glotfelter, S. Wilson, G. Notomista, and M. Egerstedt, "Data-driven robust barrier functions for safe, long-term operation," *IEEE Trans. Robot.*, vol. 38, no. 3, pp. 1671–1685, Jun. 2022.

[34] A. Isaly, O. S. Patil, R. G. Sanfelice, and W. E. Dixon, "Adaptive safety with multiple barrier functions using integral concurrent learning," in *Proc. Amer. Control Conf.*, 2021, pp. 3719–3724.

[35] A. Alan, T. G. Molnar, E. Daş, A. D. Ames, and G. Orosz, "Disturbance observers for robust safety-critical control with control barrier functions," *IEEE Control Syst. Lett.*, vol. 7, pp. 1123–1128, 2023.

[36] Y. Wang and X. Xu, "Disturbance observer-based robust control barrier functions," in *Proc. Amer. Control Conf.*, 2023, pp. 3681–3687.

[37] E. Daş and R. M. Murray, "Robust safe control synthesis with disturbance observer-based control barrier functions," in *Proc. 61st IEEE Conf. Decis. Control*, 2022, pp. 5566–5573.

[38] J. Sun, J. Yang, and Z. Zeng, "Safety-critical control with control barrier function based on disturbance observer," *IEEE Trans. Autom. Control*, vol. 69, no. 7, pp. 4750–4756, Jul. 2024.

[39] D. R. Agrawal and D. Panagou, "Safe and robust observer-controller synthesis using control barrier functions," *IEEE Control Syst. Lett.*, vol. 7, pp. 127–132, 2023.

[40] M. Black and D. Panagou, "Safe control design for unknown nonlinear systems with Koopman-based fixed-time identification," *IFAC-PapersOnLine*, vol. 56, no. 2, pp. 11369–11376, 2023.

[41] A. Isaly, O. S. Patil, H. M. Sweatland, R. G. Sanfelice, and W. E. Dixon, "Adaptive safety with a rise-based disturbance observer," *IEEE Trans. Autom. Control*, vol. 69, no. 7, pp. 4883–4890, Jul. 2024.

[42] A. J. Taylor, V. D. Dorobantu, S. Dean, B. Recht, Y. Yue, and A. D. Ames, "Towards robust data-driven control synthesis for nonlinear systems with actuation uncertainty," in *Proc. 60th IEEE Conf. Decis. Control*, 2021, pp. 6469–6476.

[43] Z. Jin, M. Khajenejad, and S. Z. Yong, "Robust data-driven control barrier functions for unknown continuous control affine systems," *IEEE Control Syst. Lett.*, vol. 7, pp. 1309–1314, 2023.

[44] J. Zheng, T. Dai, J. Miller, and M. Sznaier, "Robust data-driven safe control using density functions," *IEEE Control Syst. Lett.*, vol. 7, pp. 2611–2616, 2023.

[45] F. Castañeda, J. J. Choi, B. Zhang, C. J. Tomlin, and K. Sreenath, "Pointwise feasibility of Gaussian process-based safety-critical control under model uncertainty," in *Proc. 60th IEEE Conf. Decis. Control*, 2021, pp. 6762–6769.

[46] A. Clark, "Control barrier functions for stochastic systems," *Automatica*, vol. 130, 2021, Art. no. 109688.

[47] A. Lederer, A. J. O. Conejo, K. A. Maier, W. Xiao, J. Umlauft, and S. Hirche, "Gaussian process-based real-time learning for safety critical applications," in *Proc. 38th Int. Conf. Mach. Learn.*, 2021, vol. 139, pp. 6055–6064.

[48] P. Mestres, K. Long, N. Atanasov, and J. Cortés, "Feasibility analysis and regularity characterization of distributionally robust safe stabilizing controllers," *IEEE Control Syst. Lett.*, vol. 8, pp. 91–96, 2024.

[49] R. K. Cosner, P. Culbertson, A. J. Taylor, and A. D. Ames, "Robust safety under stochastic uncertainty with discrete-time control barrier functions," in *Proc. Robot.: Sci. Syst. XIX*, 2023.

[50] K. Long, V. Dhiman, M. Leok, J. Cortés, and N. Atanasov, "Safe control synthesis with uncertain dynamics and constraints," *IEEE Robot. Automat. Lett.*, vol. 7, no. 3, pp. 7295–7302, Jul. 2022.

[51] P. S. Oruganti, P. Naghizadeh, and Q. Ahmed, "Robust control barrier functions for sampled-data systems," *IEEE Control Syst. Lett.*, vol. 8, pp. 103–108, 2024.

[52] S. Dean, A. J. Taylor, R. K. Cosner, B. Recht, and A. D. Ames, "Guaranteeing safety of learned perception modules via measurement-robust control barrier functions," in *Proc. Conf. Robot. Learn.*, 2021, pp. 654–670.

[53] P. Seiler, M. Jankovic, and E. Hellstrom, "Control barrier functions with unmodeled input dynamics using integral quadratic constraints," *IEEE Control Syst. Lett.*, vol. 6, pp. 1664–1669, 2021.

[54] C. I. Chinelato and B. A. Angélico, "Robust exponential control barrier functions for safety-critical control," in *Proc. Amer. Control Conf.*, 2021, pp. 2342–2347.

[55] J. Peng, H. Wang, S. Ding, J. Liang, and Y. Wang, "Robust high-order control barrier functions-based optimal control for constrained nonlinear systems with safety-stability perspectives," *IEEE Trans. Automat. Sci. Eng.*, vol. 21, no. 4, pp. 4948–4958, Oct. 2024.

[56] L. Perko, *Differential Equations and Dynamical Systems*. Berlin, Germany: Springer, 2013.

[57] F. Blanchini and S. Miani, *Set-Theoretic Methods in Control*. Berlin, Germany: Springer, 2008.

[58] M. Nagumo, "Über die lage der integralkurven gewöhnlicher differentialgleichungen," *Proc. Physico- Math. Soc. Japan. 3rd Ser.*, vol. 24, pp. 551–559, 1942.

[59] M. H. Cohen, T. G. Molnar, and A. D. Ames, "Safety-critical control for autonomous systems: Control barrier functions via reduced-order models," *Annu. Rev. Control*, vol. 57, 2024, Art. no. 100947.

[60] A. D. Ames, X. Xu, J. W. Grizzle, and P. Tabuada, "Control barrier function based quadratic programs for safety critical systems," *Trans. Autom. Control*, vol. 62, no. 8, pp. 3861–3876, 2017.

[61] M. Alyaseen, N. Atanasov, and J. Cortés, "Continuity and boundedness of minimum-norm CBF-safe controllers," *IEEE Trans. Automatic Control*, early access, Jan. 17, 2025, doi: 10.1109/TAC.2025.3531774.

[62] A. Alan, A. J. Taylor, C. R. He, A. D. Ames, and G. Orosz, "Control barrier functions and input-to-state safety with application to automated vehicles," *IEEE Trans. Control Syst. Technol.*, vol. 31, no. 6, pp. 2744–2759, Nov. 2023.

[63] T. G. Molnar, G. Orosz, and A. D. Ames, "On the safety of connected cruise control: Analysis and synthesis with control barrier functions," in *Proc. 62nd IEEE Conf. Decis. Control*, 2023, pp. 1106–1111.

[64] N. Weaver, *Lipschitz Algebras*. Singapore: World Scientific, 2018.

[65] X. Xu, P. Tabuada, J. W. Grizzle, and A. D. Ames, "Robustness of control barrier functions for safety critical control," *IFAC-PapersOnLine*, vol. 48, no. 27, pp. 54–61, 2015.

[66] A. Alan, T. G. Molnar, A. D. Ames, and G. Orosz, "Parameterized barrier functions to guarantee safety under uncertainty," *IEEE Control Syst. Lett.*, vol. 7, pp. 2077–2082, 2023.

[67] A. J. Taylor, V. D. Dorobantu, S. Dean, B. Recht, Y. Yue, and A. D. Ames, "Towards robust data-driven control synthesis for nonlinear systems with actuation uncertainty," in *Proc. 60th IEEE Conf. Decis. Control*, 2021, pp. 6469–6476.

[68] E. Das and J. W. Burdick, "Robust control barrier functions using uncertainty estimation with application to mobile robots," 2024, *arXiv:2401.01881*.

[69] R. Sinha, J. Harrison, S. M. Richards, and M. Pavone, "Adaptive robust model predictive control with matched and unmatched uncertainty," in *Proc. Amer. Control Conf.*, 2022, pp. 906–913.

[70] J. Breeden and D. Panagou, "Robust control barrier functions under high relative degree and input constraints for satellite trajectories," *Automatica*, vol. 155, 2023, Art. no. 111109.

[71] T. Gurriet, M. Mote, A. Singletary, P. Nilsson, E. Feron, and A. D. Ames, "A scalable safety critical control framework for nonlinear systems," *IEEE Access*, vol. 8, pp. 187249–187275, 2020.

[72] D. E. van Wijk, S. Coogan, T. G. Molnar, M. Majji, and K. L. Hobbs, "Disturbance-robust backup control barrier functions: Safety under uncertain dynamics," *IEEE Control Syst. Lett.*, vol. 8, pp. 2817–2822, 2024.

[73] A. Domahidi, E. Chu, and S. Boyd, "ECOS: A SOCP solver for embedded systems," in *Proc. Eur. Control Conf.*, 2013, pp. 3071–3076.

[74] R. Strongin, "On the convergence of an algorithm for finding a global extremum," *Eng. Cybern.*, vol. 11, pp. 549–555, 1973.

[75] G. Wood and B. Zhang, "Estimation of the Lipschitz constant of a function," *J. Glob. Optim.*, vol. 8, pp. 91–103, 1996.

[76] A. K. Kiss, T. G. Molnar, A. D. Ames, and G. Orosz, "Control barrier functionals: Safety-critical control for time delay systems," *Int. J. Robust Nonlinear Control*, vol. 33, no. 12, pp. 7282–7309, 2023.

[77] T. Insperger and R. Horváth, "Pendulum with harmonic variation of the suspension point," *Periodica Polytechnica Mech. Eng.*, vol. 44, no. 1, pp. 39–46, 2000.

[78] A. Luongo and A. Casalotti, "Asymptotic analysis of circular motions of base-and length-parametrically excited pendula," *Nonlinear Dyn.*, vol. 112, no. 2, pp. 757–773, 2024.

ANIL ALAN (Student Member, IEEE) received the B.Sc. degree from Mechanical Engineering Departments of Middle East Technical University, Ankara, Türkiye, in 2012, the M.Sc. degree from Bilkent University, Ankara, in 2017, and the Ph.D. degree from the University of Michigan, Ann Arbor, MI USA, in 2024. He is currently a Postdoc with the Delft University of Technology, Delft, The Netherlands. His research focuses on nonlinear safety-critical control with application to connected automated vehicles.

TAMAS G. MOLNAR (Member, IEEE) received the B.Sc. degree in mechatronics engineering, the M.Sc., and Ph.D. degrees in mechanical engineering from the Budapest University of Technology and Economics, Budapest, Hungary, in 2013, 2015, and 2018, respectively. He was a Postdoc with the University of Michigan, Ann Arbor, MI, USA, from 2018 to 2020, and the California Institute of Technology from 2020 to 2023. Since 2023, he has been an Assistant Professor of mechanical engineering with Wichita State University, Wichita, KS, USA. His research interests include nonlinear dynamics and control, safety-critical control, and time delay systems with applications to connected automated vehicles, robotic systems, and autonomous systems.

AARON D. AMES (Fellow, IEEE) received the joint B.S. degree in mechanical engineering and B.A. degree in mathematics from the University of St. Thomas, St Paul, MN, USA, in 2001, and the joint M.A. degree in mathematics and the Ph.D. degree in electrical engineering and computer sciences from the University of California (UC), Berkeley, Berkeley, CA USA, in 2006. He was an Associate Professor with Georgia Tech, Woodruff School of Mechanical Engineering, Atlanta, GA, USA, and the School of Electrical & Computer Engineering, Atlanta. He is the Bren Professor of mechanical and civil engineering and control and dynamical systems with Caltech. He was a Postdoctoral Scholar in control and dynamical systems with Caltech from 2006 to 2008, and began his faculty career with Texas A&M University, Texas, TX, USA, in 2008. His research interests include the areas of robotics, nonlinear, safety-critical control, and hybrid systems, with a special focus on applications to dynamic robots, both formally and through experimental validation. At UC Berkeley, he was the recipient of the 2005 Leon O. Chua Award for achievement in nonlinear science and the 2006 Bernard Friedman Memorial Prize in Applied Mathematics, NSF CAREER Award in 2010, 2015 Donald P. Eckman Award, and 2019 IEEE CSS Antonio Ruberti Young Researcher Prize.

GÁBOR OROSZ (Senior Member, IEEE) received the M.Sc. degree in engineering physics from the Budapest University of Technology, Budapest, Hungary, in 2002, and the Ph.D. degree in engineering mathematics from the University of Bristol, Bristol, U.K., in 2006. He held postdoctoral positions with the University of Exeter, Exeter, U.K., and with the University of California, Santa Barbara, Santa Barbara, CA, USA. In 2010, he joined the University of Michigan, Ann Arbor, MI, USA, where he is currently a Professor of mechanical engineering and in civil and environmental engineering. From 2017 to 2018, he was a Visiting Professor of control and dynamical systems with the California Institute of Technology, Pasadena, CA. In 2022, he was a Distinguished Guest Researcher in applied mechanics with the Budapest University of Technology, where he was a Fulbright Scholar. His research interests include nonlinear dynamics and control, time delay systems, machine learning, and data-driven systems with applications to connected and automated vehicles, traffic flow, and biological networks.